UNIVERSIDADE DE LISBOA
FACULDADE DE MOTRICIDADE HUMANA

UNIVERSIDADE DE LISBOA
FACULDADE DE MOTRICIDADE HUMANA

# Comparison of sonographic techniques for the assessment of biceps femoris long head architecture

Dissertação elaborada com vista à obtenção
do Grau de Mestre em Treino de Alto Rendimento

Orientador:

Doutor Sandro Remo Martins Neves Ramos Freitas

Júri:

Doutor Anthony John Blazevich
Doutora Filipa Oliveira da Silva João

**Ricardo Jorge Lemos Pimenta**

Lisboa, 2018

# AGRADECIMENTOS

Em primeiro lugar, gostaria de salientar que desde jovem a obtenção deste mestrado passava pelos meus planos. Na infância comecei a minha ligação com o desporto, nomeadamente o futebol, com o passar dos anos comecei a querer entender como poderia melhorar o meu rendimento. Nessa altura, as pesquisas eram bem diferentes das de agora, mas o objetivo foi sempre o mesmo, tornar-me um profissional de excelência no ramo do treino de alto rendimento. Desta forma, para estar no caminho da excelência só faria sentido entrar para este mestrado.

A concretização deste feito, deve-se essencialmente a todas as condições que os meus pais me conseguiram proporcionar até estar aqui presente. Assim sendo, o primeiro agradecimento é dirigido em conjunto, aos meus pais. Agradecer à minha mãe por todo o apoio demonstrado ao longo desta caminhada, estando sempre do meu lado nas decisões que tomei. Agradecer ao meu pai, por todos os valores que me transmitiu e incutiu desde criança. De realçar, valores que foram importantes para esta jornada, como a resiliência, ambição e postura de trabalhador. Estas duas pessoas são os pilares da minha vida e que se este grau de mestre é uma realidade, deve-se fundamentalmente a vocês. Obrigado!

Gostaria também de agradecer, ao professor Sandro, por todo a energia, motivação e apoio demonstrado ao longo do projeto. De realçar, todo o conhecimento que me transmitiu não só a nível académico, do qual estou profundamente agradecido.

## DEDICATÓRIA

*Aos meus pais, Maria Isabel Pimenta e Abel Gomes Pimenta, por serem os pilares da minha vida.*

*Ao meu avô Manuel Pimenta, que sempre foi um motivo de orgulho para mim, espero conseguir retribuir.*

*À minha avó Maria da Glória, por ser a alegria da minha vida!*

# INDEX

## TABLE INDEX

## INDEX OF FIGURES

## LIST OF ABBREVIATIONS

**BF** – Bicep femoris

**BFlh** – Bicep femoris long head

**EFOV** – Extended field-of-view

**FA** – Fascicle angle

**FL** – Fascicle length

**ICC** – Intraclass correlation coefficient

**MT** – Muscle thickness

**SEM** – Standard error of the mean

**VL** – Vastus lateralis

**MRI** – Magnetic resonance imaging

**DTI** – Diffusion tensor imaging

**MTJ** – Myotendinous junction

**ROI** – Region of interest

# RESUMO

**Objetivo:** Avaliar a repetibilidade e a concordância entre três técnicas sonográficas usadas para quantificar a arquitetura da cabeça longa do bicípite femoral (BFlh): i) imagem estática; ii) *extended field-of-view* (EFOV) com o caminho da sonda de ultrassom de forma linear (EFOV linear); e iii) EFOV com o percurso da sonda de forma não linear (EFOV não linear) para seguir as complexas trajetórias dos fascículos**.**

**Método:** Vinte sujeitos (24,4 ± 5,7 anos; 175 ± 0,8 cm; 73 ± 9,0 kg) sem historial de lesão nos isquiotibiais foram convidados a participar neste estudo. Foi utilizado um aparelho de ultrassom ligado a uma sonda linear de 6 cm, operando a uma frequência de 10 MHz para avaliar a arquitetura da BFlh em *B mode*.

**Resultados:** A sonda de ultrassom foi posicionada a 52,0 ± 5,0% do comprimento do fêmur e 57,0 ± 6,0% do comprimento da BFlh. Encontramos uma repetibilidade aceitável ao avaliar o comprimento do fascículo da BFlh ($ICC_{3,k}$ = 0,86-0,95; SEM = 1,9-3,2 mm) e ângulo de penação ($ICC_{3,k}$ = 0,85-0,97; SEM = 0,8-1,1º) em todas as três técnicas sonográficas. No entanto, a técnica EFOV não linear mostrou maior repetibilidade (comprimento do fascículo $ICC_{3,k}$ = 0,95; ângulo de penação, $ICC_{3,k}$ = 0,97). A técnica de imagem estática superestimou o comprimento do fascículo (8-11%) e subestimou o ângulo de penação (8-9%) em comparação com as técnicas de EFOV. Além disso, a ordem de classificação dos sujeitos variou em cerca de 15% entre a imagem estática e o EFOV não linear**.**

**Conclusões:** Embora todas as técnicas tenham apresentado boa repetibilidade, os erros absolutos foram observados com imagens estáticas (7,9 ± 6,1 mm para

o comprimento do fascículo) e EFOV linear (3,7 ± 3,0 mm), provavelmente porque as complexas trajetórias dos fascículos não foram acompanhadas. A ordem de classificação dos indivíduos para o comprimento e ângulo de penação também foi diferente entre a imagem estática e o EFOV não linear. Desta forma, diferentes estimativas quanto ao risco de lesão e função muscular poderiam ter sido feitas ao usar essa técnica.

**Palavras chave:** Ultrassonografia; repetibilidade; *extended fiel-of-view*; comprimento do fascículo; ângulo de penação.

# ABSTRACT

**Purpose:** To assess the repeatability of, and measurement agreement between, three sonographic techniques used to quantify biceps femoris long head (BFlh) architecture: i) static-image; ii) extended field-of-view (EFOV) with linear ultrasound probe path (linear-EFOV); and iii) EFOV with nonlinear probe path (nonlinear-EFOV) to follow the complex fascicle trajectories.

**Methods:** Twenty individuals (24.4±5.7 years; 175±0.8 cm; 73±9.0 kg) without history of hamstring strain injury were invited to participate in this study. An ultrasound scanner coupled with 6-cm linear probe operating at a 10-MHz frequency was used to assess BFlh architecture in B-mode.

**Results:** The ultrasound probe was positioned at 52.0±5.0% of femur length and 57.0±6.0% of BFlh length. We found an acceptable repeatability when assessing BFlh fascicle length ($ICC_{3,k}$ = 0.86-0.95; SEM = 1.9-3.2 mm) and angle ($ICC_{3,k}$ = 0.85-0.97; SEM = 0.8-1.1º) using all three sonographic techniques. However, the nonlinear-EFOV technique showed the highest repeatability (fascicle length $ICC_{3,k}$ = 0.95; fascicle angle, $ICC_{3,k}$ = 0.97). The static-image technique overestimated fascicle length (8-11%) and underestimated fascicle angle (8-9%) compared to both EFOV techniques. Also, the rank order of individuals varied by ~15% between static-image and nonlinear-EFOV techniques when assessing the fascicle length.

**Conclusions:** Although all techniques showed good repeatability, absolute errors were observed using static-image (7.9±6.1 mm for fascicle length) and linear-EFOV (3.7±3.0 mm), probably because the complex fascicle trajectories were not followed. The rank order of individuals for fascicle length and angle were also different between static-image and nonlinear-EFOV, so different muscle function and injury risk estimates could likely be made when using this technique.

**Key words:** ultrasonography; repeatability; extended field-of-view; fascicle length; pennation angle.

# CHAPTER I

# INTRODUCTION

# CHAPTER I – INTRODUCTION

## 1.1. Introduction to the problem

Biceps femoris long head (BFlh) crosses the knee and hip joints posteriorly, acting as both a knee flexor, hip extensor, and tibia external rotator. BFlh also presents a complex muscle architecture, possibly because of its function complexity, which is non-uniform and heterogeneous along its length (Bennett, Rider, Domire, DeVita, & Kulas, 2014; Kellis, Galanis, Natsis, & Kapetanos, 2010). The muscle fascicles follow a nonlinear (often concave-to-convex) path, are differentially orientated along the muscle length, and most, but not all, insert onto a prominent mid-belly aponeurosis (Chleboun, France, Crill, Braddock, & Howell, 2001; Kellis, Galanis, Natsis, & Kapetanos, 2009). BFlh architecture is commonly assessed *in vivo* using sonographic techniques, has been statistically associated with hamstring strain injury risk (Timmins, Bourne, et al., 2016). For instance, Timmins et al. (2016) have reported that athletes with a shorter BFlh fascicle length have greater risk for sustaining a hamstring strain injury (Timmins et al., 2016). However, previous studies assessing BFlh architecture have not accounted for the complex orientation of fascicles within the BFlh belly and have used varying sonographic procedures. It is not currently known whether these fascicle length estimates are reflective of those obtained using more complex (assumedly more accurate) methods, and thus whether these associations hold true when fascicle lengths are more accurately measured.

Amongst sonographic techniques the static-image technique is the most common (Ribeiro-Alvares, Marques, Vaz, & Baroni, 2018). Using this technique on BFlh, the ultrasound transducer is typically placed at 50% of femur length, as indicated by bony landmarks (i.e. distance between the greater trochanter and the head of the fibula), and oriented according to the fascicle

direction between the mid-belly and superficial aponeurosis (Kellis et al., 2009; Oliveira et al., 2016; Tosovic et al., 2016; Kwah, Pinto, Diong, & Herbert, 2013). However, since BFlh has a heterogeneous and non-uniform architecture, such assessment methods may not accurately capture the fascicles for two main reasons. First, the sonogram field of view may not be sufficient to capture the full fascicle length, which necessitates the need for extrapolation techniques to estimate the non-visible portion of the fascicles. Second, BFlh fascicles follow a nonlinear path, which ensures that static-image estimates would over- (for convex curvature) or under-estimate (for concave curvature) BFlh fascicle length; and, importantly to say, previous studies using the static-image technique have assumed a linear fascicle path as they have used a straight tool to identify the fascicle path (Kellis et al., 2009; Tosovic et al., 2016; Freitas et al., 2017). To overcome such limitations, the extended field-of-view (EFOV) technique has been proposed (Cooperberg, Barberie, Wong, & Fix, 2001; Noorkoiv, Stavnsbo, Aagaard, & Blazevich, 2010). However, few studies have used the EFOV technique to assess BFlh architecture (Gonçalves et al., 2017; Seymore, Domire, DeVita, Rider, & Kulas, 2017; Tosovic et al., 2016) and these studies have either not fully described the path followed by the ultrasound transducer during image capture or have used a linear transducer path (Tosovic et al., 2016), which is not appropriate to follow nonlinear fascicle paths. Since no comparison has been performed between the different ultrasound techniques in assessing the BFlh architecture, it is unknown whether a EFOV technique using either a linear or nonlinear path would give a different BFlh architectural outcomes and repeatability compared to the static-image technique.

**Study aim and hypothesis**

The aim of the present study was to compare the repeatability of, and determine the measurement agreement between, three sonographic techniques currently used to assess BFlh architecture (i.e. fascicle length and angle): i) static-image; ii) EFOV with a linear ultrasound probe path (linear-EFOV); and iii) EFOV with nonlinear ultrasound probe path (nonlinear-EFOV). We hypothesized that i) the repeatability would be higher for the static-image technique compared to the nonlinear-EFOV and linear-EFOV technique and ii) the static-image technique would underestimate BFlh fascicle length compared to the nonlinear-EFOV technique.

# CHAPTER II

# REVIEW OF LITERATURE

# CHAPTER II – REVIEW OF LITERATURE

## 2.1. Basic Concepts of Muscle Architecture

According by Otten (1988) the first work about function models and concepts of skeletal muscle architecture was published in 1664 by the Danish scientist Stensen, with a monograph entitled "Anatomical observations." Since then, new theories and informations to analyse and interpret the skeletal muscle architecture have been developed (Brand, Beach, & Thompson, 1981). Muscle architecture is defined as the arrangement of fibers within a muscle (Gans, 1982). Although other physical parameters such as muscle mass, volume and other metabolic indicator such as fiber type distribution substantially influences the contractile properties, some authors have suggested that none predicts muscle function like the muscle architecture (Burkholder, Fingado, Baron, & Lieber, 1994; Lieber & Fridén, 2000). The arguments underlying this statement will be presented further in the present manuscript. When the muscle architecture it is the focus of the question, terms as fascicle length (FL), fascicle angle (FA) (i.e. also named pennation angle), and muscle thickness (MT) are called into the question (Fig. 1).

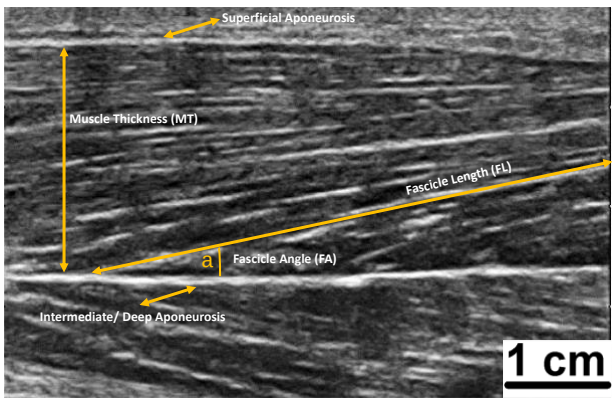


**Figure 1**. Identification of the three main outcomes derived from the skeletal muscle architecture assessment, from a sonogram taken at the mid-distance of the femur length, in the back of the thigh, and capturing the biceps femoris long head: deep aponeurosis, fascicle angle, fascicle length, muscle thickness, and superficial aponeurosis.

The FL and the FA are the most studied variables (Abe, Kumagai, & Brechue, 2000; Tetsuo Fukunaga, Ichinose, Ito, Kawakami, & Fukashiro, 1997; Kawakami, Abe, & Fukunaga, 1993; Otten, 1988; Rutherford & Jones, 1992). However, there is a certain discrepancy in previous studies regarding the method used to perform the measurements. For instance, for the FL measurements in vastus lateralis, (T. Fukunaga, Kawakami, Kuno, Funato, & Fukashiro, 1997) determined the FL as the length of a line drawn along the ultrasonic echo parallel to fascicles (which was considered as fibers as well), from their proximal and distal ends. On other hand (Abe et al., 2000), determined the fascicle length from a formula which included the isolate muscle thickness (i.e. distance between subcutaneous adipose tissue-muscle interface and intermuscular interface) and fascicle angle (1):

$$FL = \text{isolated muscle thickness} \bullet \sin\alpha^{-1} \quad (1)$$

For Tosovic, Muirhead, Brown, & Woodley (2016), the FL of BFLh was defined as the length of an entire muscle fascicle that extends from the superficial aponeurosis to the deep intramuscular aponeurosis. In this document, the FL was considered as a group of fibers involved by a perimysial conjunctival fraction that extends between two aponeuroses. Therefore, the FL length was considered as the distance between the insertions of the FL onto the aponeurosis by following the FL path. Important to note that as the FL orientation implies the orientation of the muscle fibers that it contains, FL may be considered an estimator of fiber length.

In respect to the FA assessment, previous studies have also used different criteria when assessing different muscles. Fukunaga in 1997 considered the FA was the angle between the echoes of the deep aponeurosis of the vastus lateralis and the echoes from interspaces among fascicles (Tetsuo Fukunaga et al.,

1997; Otten, 1988). Other studies also used this definition (Abe et al., 2000; Tetsuo Fukunaga et al., 1997; Kawakami et al., 1993; Rutherford & Jones, 1992). In other perspective, other studies digitized two points on each fascicle, one 3 mm from the deep aponeurosis and the second at 50% of the distance from the deep to superficial aponeurosis (Blazevich, Cannavan, Coleman, & Horne, 2007; Timmins, Shield, Williams, Lorenzen, & Opar, 2015). As mentioned by the studies authors, this allowed accurate delineation of the fascicles without incorporating the slightly greater fascicle curvature that can occur at the insertion point of the fascicles on the deep aponeurosis. For Tosovic et al. (2016), the fascicle angle was defined as the angle between the superficial aponeurosis and a clearly visible fascicle, measured using the angle tool of the ImageJ software (National Institutes of Health, Bethesda, MD), without precising where fascicle was digitized. This indicates that a different aponeurosis could be considered when assessing the FA, as well the sites where the fascicle is digitized. In this study, we describe the FA as the angle between the fascicle orientation (i.e. defined by the most superficial and deep insertions sites onto the aponeuroses) and the deep aponeurosis, considering that the aponeurosis is aligned to the muscle line of action during contraction (Timmins, Shield, Williams, Lorenzen, & Opar, 2015). The aponeurosis is defined as a multilayered structure with densely laid down bundles of collagen with major preferential directions, that extends from the tendon, and contains insertions of muscle fascicles (Huijing PhD, Huijing, & Langevin, 2009). Note that the epimysium also covers the aponeurosis but is not attached to them.

The arrangement of the muscle fibers and them insertion (or not) in the aponeurosis, modified the name of type for muscle architecture. The human skeletal muscle can be described as either parallel or pennate. In parallel muscles, the fibers run parallel to the line of pull of the muscle. In pennate muscles, fibers run obliquely to the axis of pull and insert into the aponeurosis

or tendon by forming an angle, called the FA or pennation angle (M. Narici, 1999). The FA, and the amount of force actually exerted on the tendon, can be calculated using the cosine of the angle of insertion. At rest, the angle of pennation in most human muscles is about 10° or less and does not appear to have a marked effect on most functional properties such as force production (Wickiewicz, Roy, Powell, & Edgerton, 1983; Wickiewicz, Roy, Powell, Perrine, & Edgerton, 1984). However, during muscle contraction the FA can vary and may change some functional parameters, at least in some muscles (Tetsuo Fukunaga et al., 1997). The pennate muscles offers a force advantage over parallel muscles, because with pennation there are more fibers in parallel for a given muscle volume, which increases the physiological cross sectional area (the area of the cross section of a muscle perpendicular to its fibers, generally at its largest point). This allows to have more sarcomeres to be arranged in parallel, resulting in enhanced force production (Gans & Gaunt, 1991; Sacks & Roy, 1982). From a functional perspective, is important to note that the force exerted by muscle fibers is modified by their geometric arrangement, structures of the joint, the angle and location of the tendon in relation to the bone (Gans & de Vree, 1987).

There are some methodological considerations when assessing the FA and FL in human skeletal muscles. For instance, the FA and FL measurement depends on the degree of muscle lengthening and muscle activity (Huijing, 1985; Muhl, 1982). Thus, it is fundamental to control for the degree of muscle activation and joint positioning during the FL and FA assessments. Also, previous studies reported the fascicles may present curvatures at rest (Blazevich et al., 2007; Tetsuo Fukunaga et al., 1997; Noorkoiv, Stavnsbo, Aagaard, & Blazevich, 2010); and, in some cases, a doubled curvature can exist (Bolsterlee, D'Souza, Gandevia, & Herbert, 2017).

The MT has been defined as the perpendicular distance between two aponeuroses within a muscle (Blazevich et al., 2007; Timmins et al., 2015). This parameter reflects muscle size. Previous studies have demonstrated that the muscle size, determined as anatomical or physiological cross-sectional area and muscle volume, is closely related to the maximal voluntary strength in isometric contractions (R. Akagi et al., 2009; Ryota Akagi et al., 2011; Maughan, Watson, & Weir, 1983).

### 2.2. Overview of Current Methods

In order to answer the problems of measuring muscular architecture, science has evolved over the years. The first skeletal muscle architecture measurements have been made with *ex vivo* animal models. According to Denny-Brown (1929) the dissection on animals started at 1678 with Stefano Lorenzini, which mentioned the striking difference in colour between certain muscles of the limb in the rabbit. After that, and according to Friederich & Brand (1990), new important studies have been published regarding the cross sectional area assessment, as the Weber work in 1846. The type of animal models to be dissected has varied along the time, using animals as rats, cats, and kangaroos (Close, 1964; Denny-Brown, 1929; Hoffer, Caputi, Pose, & Griffiths, 1989; Morgan, Proske, & Warren, 1978); and, only years after, started to be performed assessments in skeletal muscles of human cadavers (Fig.2) (Brand et al., 1981; Friederich & Brand, 1990; Wickiewicz et al., 1983). The dissection was the first method developed to analyse the muscle architecture. This method consists on the dismembering of the body of a deceased (i.e. animal, plant or human) to study the anatomy. The main advantage of the dissection is that allows to understand and visualize *in loco*

the composition/tissues of the body by avoiding structures that should not be evaluated (Friederich & Brand, 1990). On the other hand, the dissection only allows to use one time the dissected animals (i.e. when the animals are sacrificed or have to be deeply anaesthetized) (Hoffer et al., 1989; Morgan et al., 1978). In humans, the dissection must be previously allowed in order to have assess and examine human cadavers, depend (of course) of their availability, and most of them are older (Friederich & Brand, 1990; Tosovic, Muirhead, Brown, & Woodley, 2016b; Wickiewicz et al., 1983).

In the middle of the 20$^{th}$ century, the sonography was proposed to be appropriate to assess the skeletal muscle architecture *in vivo*, and non-invasively (Ikai & Fukunaga, 1968). To our knowledge, (Ikai & Fukunaga, 1968) reported the first sonographic study that proposed to assess the skeletal muscle morphology, measuring the cross section area. Since then, the quality of ultrasound measures have improved (Gary S. Chleboun, France, Crill, Braddock, & Howell, 2001; Dons, Bollerup, Bonde-Petersen, & Hancke, 1979; Tetsuo Fukunaga et al., 1997; Heckmatt, Dubowitz, & Leeman, 1981; Noorkoiv et al., 2010) until now (Kellis, 2018; Seymore, Domire, DeVita, Rider, & Kulas, 2017; Tosovic et al., 2016). Currently, the ultrasonography is considered an usual and appropriate method in medicine (by using echo waves through high frequency ultrasound) to visualize, in real time, the internal structures of the body.

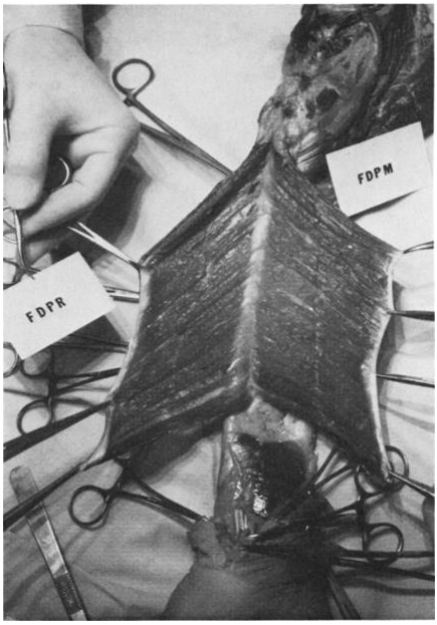


**Figure 2**. Desiccation of flexor digitorum profundus to middle finger (FDPM) and ring fingers (FDPR). Image taken from Brand, Beach, and Thompson 1981.

Parallel to the ultrasound measurements, discoveries of muscle architecture have been also performed using magnetic resonance imaging (Cleveland, Chang, Hazlewood, & Rorschach, 1976). The magnetic resonance imaging (MRI) is currently widely considered to be the gold standard for the muscle morphological assessment *in vivo* due to the high contrast between tissues of different molecular properties, by using the diffusion tensor imaging (DTI) (P. J. Basser, Mattiello, & LeBihan, 1994). The measurement of an effective diffusion tensor of water in tissues can provide clinically relevant information that is not available from other imaging modalities (Peter J. Basser & Jones, 2002). This information includes parameters that help to characterize physical

properties of tissue constituents, tissue microstructure, and architectural organization.

Thus, the DTI provides a good approach for determining the muscle shape and the orientation of the muscle fibers, which are assumed to be similar to the fascicles (Fig.3) (Budzik et al., 2007; Giraudo et al., 2018). DTI is based on the correspondence between the principal direction of water diffusion and the local cellular geometry in tissues such as skeletal muscle (Cleveland et al., 1976; Damon, Ding, Anderson, Freyer, & Gore, 2002; Henkelman, Mark Henkelman, Stanisz, Kim, & Bronskill, 1994), cardiac muscle (Wu et al., 2006), the white matter tracts of the central nervous system (P. J. Basser & Pierpaoli, 1996), and have found clinical application in neuroradiology (Yang, Zhang, Zhang, Zhao, & Zhao, 2006). It has been demonstrated that DTI fiber tracking is feasible in human muscle studies as well (Sinha, Sinha, & Edgerton, 2006). DTI may additionally be useful for studies of the musculoskeletal field (Budzik et al., 2007) as muscle microarchitecture, with potential sensitivity to such parameters as fiber diameter (Galbán, Maderwald, Uffmann, de Greiff, & Ladd, 2004; Saotome, Sekino, Eto, & Ueno, 2006), and muscle injury (Heemskerk et al., 2006; Zaraiskaya, Kumbhare, & Noseworthy, 2006). So DTI, offers great potential for understanding structure-function relationships in human skeletal muscles (Lansdown, Ding, Wadington, Hornberger, & Damon, 2007). However, the access to DTI for research purposes is often limited due to the large clinical demand and the considerable cost. Consequently, other alternative methods, as sonography, is more often used.

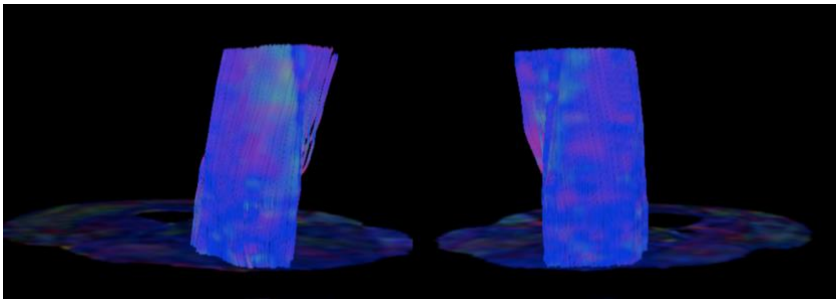

**Figure 3.** Corresponding fiber tracking of semitendinosus muscles at the mid-thigh, the left (left side) and right (right side) thighs. Image taken from Giraudo et al., 2018.

### 2.3. Assessment using Sonography

The diagnostic sonography (ultrasonography) is an imaging technique used to visualize subcutaneous body structures including tendons, muscles, joints, vessels and internal organs for possible pathology or lesions. The mechanism underlying the sonography is complex. Briefly, the ultrasound machine incorporates a transducer to perform the scans that originates the sound to be transmitted with a very high frequency into the body. A water-based gel is often placed between the patient's skin and the probe in order to improve the acoustic condition. The sound wave generated when propagates into the tissues is partially reflected from the layers between different tissues. Specifically, sound is reflected anywhere there are density changes in the body (e.g. blood cells in blood plasma, small structures in organs, etc). Some of the reflections return to the transducer. The return of the sound wave to the transducer results in the same process that it takes to emit the sound wave, but with an opposite direction. The return of the sound wave vibrates the transducer, and the transducer converts the vibrations into electrical pulses that travel to the ultrasonic scanner where they are processed and transformed into a digital image (Fig. 4-A) (Jauhiainen, 2009).

Typical diagnostic sonographic scanners operate in the frequency range of 2 to 18 megahertz (MHz), which is hundreds of times greater than the limit of human hearing. Note that, if the frequency is higher, more superficial tissues will be the scanned. For the assessment of muscle architecture, the probe normally operates at 10-12 MHz (Freitas, Marmeleira, Valamatos, Blazevich, & Mil-Homens, 2017; Kellis, 2018; Timmins, Bourne, et al., 2016a; Timmins et al., 2015). The sonography has been the front-line technique for investigating musculoskeletal architecture in different areas, because of its accessibility and reduced cost (Connell et al., 2004).

Ultrasonography has been used to measure changes in MT (Hides, Stokes, Saide, Jull, & Cooper, 1994; Misuri et al., 1997), FA (Herbert & Gandevia, 1995; Maganaris & Baltzopoulos, 1999), and FL (McKenzie, Gandevia, Gorman, & Southon, 1994; M. V. Narici et al., 1996), in different conditions as during static and dynamic contractions (Blackburn, Troy Blackburn, & Pamukoff, 2014; Ribeiro-Alvares, Marques, Vaz, & Baroni, 2018; Cepeda, Lodovico, Fowler, & Rodacki, 2015; Hodges, Pengel, Herbert, & Gandevia, 2003; Timmins, Bourne, et al., 2016b; Timmins, Shield, Williams, Lorenzen, & Opar, 2015), or during passive muscle stretching (Kellis, 2018; Nakamura, Ikezoe, Takeno, & Ichihashi, 2013). Ultrasonography has also been suggested to be able to noninvasively record the activity from deep muscles without crosstalk from adjacent muscles; but, with limited data to validate such proposal (Hodges et al., 2003). The ultrasonography method is a valid and reliable alternative tool for assessing cross-sectional areas of large individual human muscles (Reeves, Maganaris, & Narici, 2004), with the probe in a transversal position to the muscle length (Fig. 4-B). This technique, however, is not of sufficient quality to allow delineation of individual muscles (Reeves et al., 2004). The FL and FA are two architectural variables that are readily

measured using ultrasound imaging. But, to not interfere with the results, little pressure on the skin should be made by the probe (Gary S. Chleboun et al., 2001). Here, the probe should be positioned in a longitudinal plan in relation to the muscle length as is shown above in figure 1. Previous studies have demonstrated that the ultrasound measurement of FA is underestimated, when compared to assessment using a DT-MRI technique (Bolsterlee, Veeger, van der Helm, Gandevia, & Herbert, 2015).

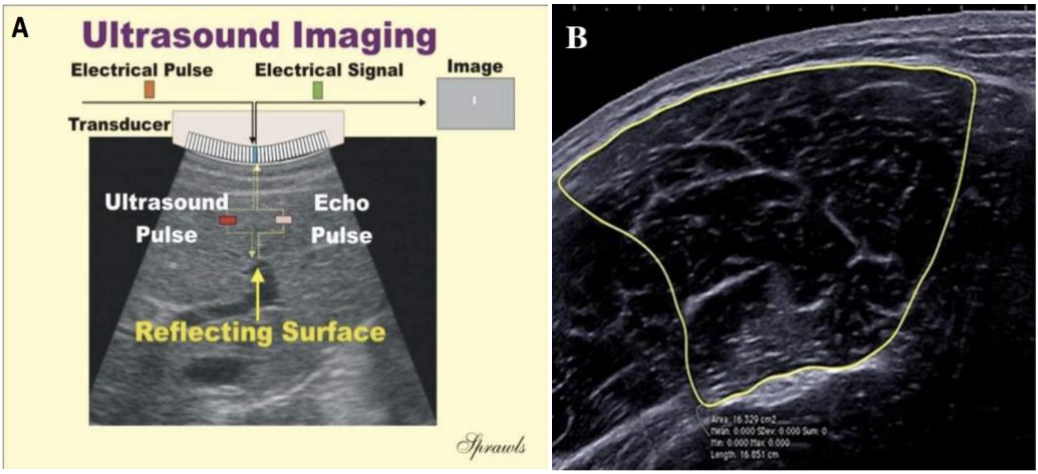


**Figure 4**. (A) Schematic representation of the mechanism underlying the sonographic measurement. Image taken from Jukka Jauhiainen 2009. (B) Cross sectional area of biceps femoris long head. Image taken from Seymore et al. 2017.

### 2.4. Biceps Femoris Long Head

#### 2.4.1. Clinical Relevance

Hamstring strains are common injuries in sport, particular in those who involve sprinting and jumping (Garrett, Califf, & Bassett, 1984; Stanton & Purdam, 1989). For instance, (Woods et al., 2004) reported a detailed analysis in English professional football players over two seasons, which 12% of all

injuries reported were hamstring strains, this being the most prevalent injury. Athletes were 2.5 times more likely to sustain a hamstring strain than a quadriceps strain during a game (Woods et al., 2004). Of the total injuries over the two seasons, nearly half (i.e. 53%) involved the biceps femoris (Woods et al., 2004). Most strains in dynamic movements of the lower limb are reported to occur in the BFlh (Brockett, Morgan, & Proske, 2004; Hoskins & Pollard, 2005; Orchard, Seward, & Orchard, 2013; Proske, Morgan, Brockett, & Percival, 2004), and the majority are recurrent (Croisier, Forthomme, Namurois, Vanderthommen, & Crielaard, 2002; Orchard et al., 2013; Verrall, Slavotinek, Barnes, Fon, & Esterman, 2006). Nonetheless, the hamstring strain injuries represent between 11 and 21.5% of the total injuries in soccer and up to 84% of the strains involved the biceps femoris, particularly the long head, while semimembranosus and semitendinosus were affected in 12% and 4% of the cases, respectively (Ekstrand, Lee, & Healy, 2016; Turner et al., 2014; Woods et al., 2004a). The region more affected is reported to be the proximal component, near to the MTJ (De Smet & Best, 2000; Silder, Heiderscheit, Thelen, Enright, & Tuite, 2008; Silder, Reeder, & Thelen, 2010).

Several factors are reported to increase the likelihood of hamstrings strains, including their two-joint anatomy and their forceful activation during eccentric contractions (Opar, Williams, & Shield, 2012; Thelen et al., 2005). Despite the frequency of hamstring muscle injuries during sprinting, it remains unclear when in the gait cycle the muscle is injured or why the BFlh is more susceptible to injury. Late swing (Wood, 1987) and early stance phases (Mann & Sprague, 1980) of sprinting have been suggested as potentially injurious phases of the gait cycle. During late swing, the hip is flexed, and the knee is extending. The hamstring muscles are active at this stage (Kuitunen, Komi, & Kyröläinen, 2002; Mero & Komi, 1987) while lengthening, which could induce an eccentric contraction injury (Garrett, 1996). Therefore, (Thelen et al., 2005)

analysis the kinematics of the hamstring muscles during treadmill sprinting and concluded that intermuscle differences in hamstring moment arms about the hip and knee may be a factor contributing to the greater propensity for hamstring strain injuries to occur in the BFlh.

An unresolved issue with hamstring strain injury is the elevated risk of recur. It has been suggested that a premature return to play (Croisier et al. 2002; Agre 1985; Jönhagen, Németh, and Eriksson 1994), or an inappropriate rehabilitation programme (Croisier et al. 2002; Agre 1985; Bennell et al. 1998), may be responsible for reinjury. But, BFlh architecture has also been statistically associated for the strain injury risk (Seymore, Domire, DeVita, Rider, & Kulas, 2017; Thelen et al., 2005; Woods et al., 2004). A previous study reported shorter fascicles have previously been associated a greater risk of injury (Timmins, Bourne, et al., 2016). Here, the eccentric strength training has became an effective method for prevention (Arnason, Andersen, Holme, Engebretsen, & Bahr, 2008; Askling, Karlsson, & Thorstensson, 2005), since it been demonstrated to increase FL and to reduce FA (Potier, Alexander, & Seynnes, 2009; Timmins, Ruddy, et al., 2016).

### 2.4.2. General Anatomy

Morphological data pertaining to BFlh have been reported in several studies (Kellis, Galanis, Natsis, & Kapetanos, 2010; Makihara, Nishino, Fukubayashi, & Kanamori, 2005; Seidel, Seidel, Gans, & Dijkers, 1996; van der Made et al., 2015; Woodley & Mercer, 2005). However, few have focused on segmental architecture (Kellis et al., 2010; Woodley & Mercer, 2005), and most data have been derived from linear measures in cadaver specimens.

The BFlh posteriorly crosses the knee and hip joints, with the proximally insertion in the ischial tuberosity and insert distally on the head of the fibula. Acts as both a knee flexor, hip extensor, and tibia external rotator. BFlh consists of two regions, a surface and a deeper one, arranged in parallel, that is separated by a mid-aponeurosis (Woodley & Mercer, 2005). BFlh presents a complex muscle architecture, which is non-uniform and heterogeneous (Bennett, Rider, Domire, DeVita, & Kulas, 2014; Kellis et al., 2010). The muscle fascicles have a non-linear path at rest and a different orientation along the muscle length, and most, but not all, fascicles inserting onto the mid-belly aponeurosis (G. S. Chleboun, France, Crill, Braddock, & Howell, 2001a; Kellis, Galanis, Natsis, & Kapetanos, 2009). The architecture of BFlh is heterogeneous in relation to the entire length of the muscle (Fig.5), by having a different behavior at different muscle activation levels (Bennett et al., 2014). Fascicles are more longer, and the FA are greater in the proximal region, compared to the distal region (Seymore et al., 2017). At rest (i.e. non-contracted condition), fascicles are thought to be curved and oriented in three planes (Freitas et al., 2017; Froeling et al., 2015). The highest BFlh cross-sectional area and muscle thickness can be found between 40-60% of the muscle length (Seymore et al., 2017).

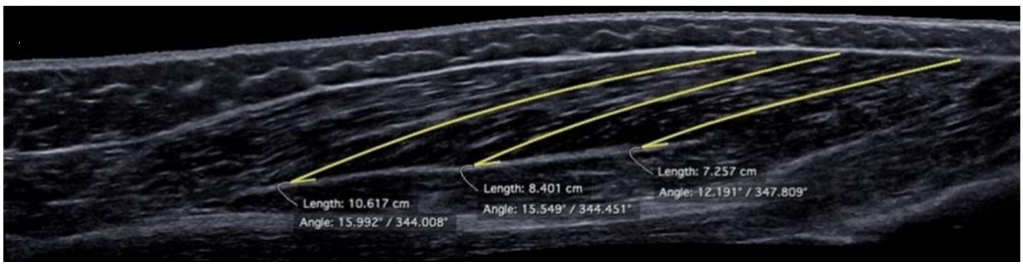


**Figure 5**. Sonogram obtained from the BFlh using ultrasonography. Right side corresponds to the distal component of BFlh. Image taken from Seymore et al. 2017.

### 2.4.3. Architecture

As already reported in the previous topic, and assuming the complexity of BF, previous studies reported that longitudinal mid-muscle aponeurosis extends from the proximal to the distal MTJ, onto which superficial fascicles insert (Kellis, Galanis, Natsis, & Kapetanos, 2009. At rest, this aponeurosis presents a non-linear path, even though the superficial BF aponeurosis follows a linear path for most of the length of the muscle belly. The proximal and distal BFlh muscle-tendon junctions have a different morphology. The distal BF muscle-tendon junction is superficial, close to the skin, and its most distal point is easily observed as it ends proximal to the biceps femoris (Freitas et al., 2017). The proximal BF muscle-tendon junction is located deep, merges medially onto the semitendinosus tendon and together insert onto the ischial tuberosity.

Tosovic in 2016 measured the BFlh using a human cadaver specimen and ultrasound reported that muscle architecture was variable throughout the BFlh length. Of note, the distal-most part of the muscle (i.e. at 90% of muscle length) contained shorter fascicles which were more pennated than its proximal most site (i.e. at 30% of muscle length). This arrangement of fascicles is typical of muscles designed for force production, as the pennated orientation allows for a relatively greater number of fascicles to be packed in the muscle, parallel to each other (Aagaard et al., 2001; Wickiewicz et al., 1983). This finding is contradictory to what was reported by (Seymore et al., 2017). This might be related to a different sonographic method used between studies. While a linear-EFOV technique was used in Tosovic (2016) study, the Seymore (2017) study do not reported the technique. Consequently, and according to (Tosovic et al., 2016) work, it appears that the proximal segment of BFlh has larger fascicle excursion potential compared to its distal region. When all the muscle architecture parameters (i.e FL, FA, and MT) were compared between the

cadaver specimens to the ultrasound measurements, lower values was noted (Tosovic et al., 2016). This could be attributed to the dehydration of the tissues.

### 2.4.4. Sonographic Considerations in Assessing the Architecture

The static-image technique is the most common to assess the BFlh architecture (Ribeiro-Alvares, Marques, Vaz, & Baroni, 2018). Using this technique, the ultrasound transducer is typically placed at 50% of femur length, as indicated by bony landmarks (i.e. distance between the greater trochanter and the head of the fibula), and usually oriented according to the fascicle direction between the superficial and mid-belly aponeurosis (Kellis, Galanis, Natsis, & Kapetanos, 2009; Oliveira et al., 2016; Tosovic et al., 2016). However, as the sonogram field of view may not be sufficient to capture the full fascicle length, and BFlh fascicles at rest have a non-linear path, the extended field of view (EFOV) technique has been proposed (Cooperberg, Barberie, Wong, & Fix, 2001; Noorkoiv et al., 2010). (Noorkoiv et al., 2010) have demonstrated a very high repeatability for the assessment of vastus lateralis FL using the EFOV ultrasonography technique.

Table 1 shows the methods and general procedures reported in previous studies that assessed the BFlh architecture using sonography, and some methodological considerations. Few studies have used the EFOV technique to assess the BFlh architecture (Bennett et al., 2014; Gonçalves, Hegyi, Avela, & Cronin, 2017; Seymore, Domire, DeVita, Rider, & Kulas, 2017c; Tosovic et al., 2016). And, these studies have either not fully described the path followed by the ultrasound transducer during image capture (Bennett et al., 2014; Gonçalves et al., 2017; Seymore et al., 2017), or have used a linear transducer path (Tosovic et al., 2016), which is not appropriate to follow nonlinear

fascicle paths. Some researchers (Gary S. Chleboun et al., 2001; Kellis et al., 2009) used a collection of images along the length of the muscle with static-image technique to reproduce all the architecture of BFlh. Regarding the location of imaging within the muscle, the region of interest (ROI) used to examine BFlh architecture has varied substantially between previous studies.

**Table 1.** Summary of the sonographic method, general procedures described in previous published studies that assessed the biceps femoris long head architecture using sonography, and some methodological considerations.

| Study& Method | General Procedures | Methodological considerations |
|---|---|---|
| Gary S. Chleboun et al., 2001<br><br>**STATIC** | "Tissue movement was recorded using two synchronized ultrasonic (US) devices (SSD-3500, ALOKA, Japan and GE LOGIQ 400 CL PRO, GE Medical Systems, U.K) with a linear array probe of 10 MHz wave frequency and a length of 6 cm (Figure 1). Muscle-tendon length was measured as the curved path from the distal origin of each muscle to the ischial tuberosity (proximal origin) using a flexible tape. The distal origin of the BFlh was set at the fibular head. For the ST, the distal tendon wraps around the knee and inserts to the fascia cruris (Figure 1)."<br><br>"Starting from the distal origin, the probe was positioned approximately at 60% of whole muscle length. This location allowed visualization of the tendinous inscription of the ST and the most proximal fascicles and intermediate tendon of the BFlh. For both probes, the angle of the probe relative to the mid-thigh line was monitored and care was taken to be standardized across testing conditions using a customized cast (Figure 1)." | Probe position at 60% of the muscle length.<br><br>Same placement of the probe for all the subjects.<br><br>Estimated the fascicle length using trigonometric extrapolation, which assumes that the fascicles are linear, ignoring the curvilinear arrangements |

| Study& Method | General Procedures | Methodological considerations |
|---|---|---|
| Kellis et al., 2009<br><br>**STATIC** | "US images were taken with the probe at approximately 10%, 30%, 50% and 70% of the curved path from the distal MTJ to the proximal origin. The angle of the probe relative to the mid-thigh line was monitored and it was standardized for all specimens." | Images in different places are better that only one image to represent all muscle length, but this method isn't valid for muscle architecture. Associated a major error.<br><br>Same placement of the probe for all the subjects.<br><br>Estimated the fascicle length using trigonometric extrapolation, which assumes that the fascicles are linear, ignoring the curvilinear arrangements. |
| Potier, Alexander, & Seynnes, 2009<br><br>**STATIC** | "The ultrasound probe (41mm, LA424 14 8, Genova, Italy) was placed on the skin overlying the distal part of the biceps femoris and its position was recorded in order to be able to replace the probe in the same position after the 8-week training period was completed. The position of the probe was recorded by measuring the distance from a fixed point on the probe to the posterior<br>margin of the iliotibial band, the greater trochanter and the tibial condyle."<br><br>"Sections of FL that were not visible on the image were extrapolated as a straight line (Maganaris et al. 1998; Narici et al. 1996), and the summation of measured and extrapolated FL was calculated to obtain total FL. | Same placement of the probe for all the subjects.<br><br>Not reported the localization of the ROI in relation to the bone and muscle length to compare the results.<br><br>Estimated the fascicle length using trigonometric extrapolation, which assumes that the fascicles are linear, ignoring the curvilinear arrangements. |

| Study& Method | General Procedures | Methodological considerations |
|---|---|---|
| Blackburn et al., 2014<br><br>**STATIC** | "Still ultrasonic images (Sonosite M-Turbo, Sonosite, Inc., Bothell, WA, USA) were obtained from the biceps femoris long head 50% of the distance between the greater trochanter of the femur and the lateral knee joint line with the muscle in a relaxed state." | Reported the probe position in relation to the muscle.<br><br>Same placement of the probe for all the subjects.<br><br>Estimated the fascicle length using trigonometric extrapolation, which assumes that the fascicles are linear, ignoring the curvilinear arrangements. |
| Cepeda, Lodovico, Fowler, & Rodacki, 2015<br><br>**STATIC** | "Since the probe was not long enough to measure fascicle length in a single image, four images of each muscle were taken and grouped."<br><br>"For the BF, the images were obtained from a site at 33% of the segment length (from the great trochanter to the articular knee line)." | Images in different places are better that only one image to represent all muscle length, but this method isn't valid for muscle architecture. Associated a major error.<br><br>Not argue the choose of ROI site.<br><br>Same placement of the probe for all the subjects.<br><br>Not reported any image for BFlh.<br><br>Estimated the fascicle length using trigonometric extrapolation, which assumes that the fascicles are linear, ignoring the curvilinear arrangements. |

| Study& Method | General Procedures | Methodological considerations |
|---|---|---|
| e Lima et al., 2015<br><br>**STATIC** | "The probe was placed at 50% of thigh length, defined as the distance from the greater trochanter to the popliteal crease."<br><br>"When the FL exceeded US field of view, FL was calculated by the extrapolation of a straight line that was summed to the visible FL, as proposed by Potier et al. Pennation angle was calculated as the acute angle formed between the deep aponeurosis and a muscle fascicle." | Use a bonymark reference and a other anatomical line.<br><br>Not reported the localization of the ROI in relation to the bone and muscle length to compare the results.<br><br>Same placement of the probe for all the subjects.<br><br>Estimated the fascicle length using trigonometric extrapolation, which assumes that the fascicles are linear, ignoring the curvilinear arrangements. |
| Freitas & Mil-Homens, 2015<br><br>**STATIC** | "A classic linear extrapolation method was used to calculate the BF architecture parameters (11). The FL was calculated using the equation: FL = L +(h/sin), where L is the observable FL from the mid-muscle aponeurosis to the most visible end point, h is the distance between the superficial aponeurosis and the fascicle visible distal end point, and b is the angle between the fascicle (drawn linearly) and the superficial aponeurosis (Figure 1B)." | Choose the most clearly area for different subjects and not the same position for all.<br><br>Not reported the localization of the probe.<br><br>Estimated the fascicle length using trigonometric extrapolation, which assumes that the fascicles are linear, ignoring the curvilinear arrangements. |

| Study& Method | General Procedures | Methodological considerations |
|---|---|---|
| Timmins et al., 2015<br><br>**STATIC** | "The scanning site was determined as the halfway point between the ischial tuberosity and the knee joint fold, along the line of the BFlh. Once the scanning site was determined, the distance of the site from various anatomical landmarks was recorded to ensure reproducibility of the scanning site for future testing sessions."<br><br>"To gather ultrasound images, the linear array ultrasound probe, with a layer of conductive gel, was placed on the skin over the scanning site, aligned longitudinally and perpendicular to the posterior thigh." | Use a bony mark reference and a anatomical line.<br><br>Not reported the localization of the ROI in relation to the bone and muscle length to compare the results.<br><br>Same placement of the probe for all the subjects.<br><br>Estimated the fascicle length using trigonometric extrapolation, which assumes that the fascicles are linear, ignoring the curvilinear arrangements. |

| Study& Method | General Procedures | Methodological considerations |
|---|---|---|
| Kellis, 2016<br><br>**STATIC** | "Tissue movement was recorded using two synchronized ultrasonic (US) devices (SSD-3500, ALOKA, Japan and GE LOGIQ 400 CL PRO, GE Medical Systems, U.K) with a linear array probe of 10 MHz wave frequency and a length of 6 cm (Figure 1). Muscle-tendon length was measured as the curved path from the distal origin of each muscle to the ischial tuberosity (proximal origin) using a flexible tape. The distal origin of the BFlh was set at the fibular head. For the ST, the distal tendon wraps around the knee and inserts to the fascia cruris (Figure 1)."<br><br>"Starting from the distal origin, the probe was positioned approximately at 60% of whole muscle length. This location allowed visualization of the tendinous inscription of the ST and the most proximal fascicles and intermediate tendon of the BFlh. For both probes, the angle of the probe relative to the mid-thigh line was monitored and care was taken to be standardized across testing conditions using a customized cast (Figure 1)." | Probe position at 60% of the muscle length.<br><br>Same placement of the probe for all the subjects.<br><br>Estimated the fascicle length using trigonometric extrapolation, which assumes that the fascicles are linear, ignoring the curvilinear arrangements. |

| Study& Method | General Procedures | Methodological considerations |
|---|---|---|
| Oliveira et al., 2016<br><br>**STATIC** | "The examiner marked one point at 50% of the length of the thigh, determined by the distance between the greater trochanter and head of the fibula."<br><br>"The probe was positioned along the direction of the fascicles, where the fascicular organization between the superficial and deep aponeurosis on the muscle was better visualized." | Only had in consideration the length of the bone and not reported % in relation to the length of the muscle.<br><br>Same placement of the probe for all the subjects.<br><br>Estimated the fascicle length using trigonometric extrapolation, which assumes that the fascicles are linear, ignoring the curvilinear arrangements. |
| Sá et al., 2016<br><br>**STATIC** | "The volunteers rested in the supine position on a stretcher. Longitudinal US images of the vastus lateralis (VL) and biceps femoris (BF) were acquired at 50% of the thigh length of the dominant leg by an experienced examiner." | Not reported any image of BFlh, only the VL.<br><br>Same placement of the probe for all the subjects.<br><br>Estimated the fascicle length using trigonometric extrapolation, which assumes that the fascicles are linear, ignoring the curvilinear arrangements. |

| Study& Method | General Procedures | Methodological considerations |
|---|---|---|
| Timmins, Bourne, et al., 2016<br><br>**STATIC** | "The scanning site was determined as the halfway point between the ischial tuberosity and the knee joint fold, along the line of the BFlh. Once the scanning site was determined, the distance of the site from various anatomical landmarks was recorded to ensure reproducibility of the scanning site for future testing sessions." | Use a bony mark reference and a anatomical line.<br><br>Same placement of the probe for all the subjects.<br><br>Not reported the localization of the ROI in relation to the bone and muscle length to compare the results.<br><br>Estimated the fascicle length using trigonometric extrapolation, which assumes that the fascicles are linear, ignoring the curvilinear arrangements. |
| Alonso-Fernandez, Docampo-Blanco, & Martinez-Fernandez, 2017<br><br>**STATIC** | "MT, FA and the estimation of FL were determined from ultrasound images obtained along the longitudinal axis of the muscle belly using a 2D B-mode ultrasound."<br><br>"The measurement site was the halfway point between the ischial tuberosity and the posterior knee joint fold, along the line of the BFlh. Once the scanning site was determined in each participant, several anatomical landmarks were taken (ischial tuberosity, fibula head and midpoint of the posterior knee joint fold) and photographs were taken in order to ensure reproducibility for future assessment sessions." | Use a the insertion of BFlh as reference and a anatomical line.<br><br>Not reported the localization of the ROI in relation to the bone and muscle length to compare the results.<br><br>Same placement of the probe for all the subjects.<br><br>Estimated the fascicle length using trigonometric extrapolation, which assumes that the fascicles are linear, ignoring the curvilinear arrangements. |

| Study& Method | General Procedures | Methodological considerations |
|---|---|---|
| Ribeiro-Alvares, Marques, Vaz, & Baroni, 2018<br><br>**STATIC** | "The scanning site for the BFlh was determined as the halfway point between the ischial tuberosity and the superior border of the fibular head."<br><br>"If necessary, slight adjustment in the probe orientation was made by the examiner in order to optimise the fascicle identification."<br><br>"Because fascicle length was greater than the probe surface, the nonvisible part was estimated through a trigonometric function." | Placement of the probe according to the length of the bone.<br><br>Same placement of the probe for all the subjects.<br><br>Estimated the fascicle length using trigonometric extrapolation, which assumes that the fascicles are linear, ignoring the curvilinear arrangements. |
| Freitas et al., 2017<br><br>**STATIC** | "The ROI was chosen in the most clearly area, capturing the superficial and mid-muscle aponeurosis and BF fascicles was obtained."<br><br>"Fascicle length was calculated using the equation: $FL=L + (h/\sin\beta)$." | Choose the most clearly area for different individuals and not the same position for all.<br><br>The static mode it is more reproducible, because the sonograms are always taken in the same position of the ROI, only variate the probe inclination but do not analyse all fascicle length.<br><br>The sonogram field of view it is not sufficient to capture the full fascicle length, which necessitates the use extrapolation techniques to estimate the non-visible component of the fascicles.<br>Estimated the fascicle length using trigonometric extrapolation, which assumes that the fascicles are linear, ignoring the curvilinear arrangements. |

| Study& Method | General Procedures | Methodological considerations |
|---|---|---|
| Kellis, 2018<br><br>**STATIC** | "This location allowed visualization of the most distal fascicles and intermediate tendon of the BFlh. Further, it was selected because distal fascicles are shorter [Kellis et al., 2012] and therefore easier to measure using US."<br><br>"In contrast, in the present study FL was determined from the distal area of the muscle using geometry estimation from US marker position data during slow passive knee joint motion. It is therefore, clear, that further research on changes in BFlh architectural parameters at various joint positions is necessary." | The location of the probe it's to much external (image in the study).<br><br>Collection of images in different regions.<br><br>Only analyze the region where the fascicles are shorter.<br><br>Estimated the fascicle length using trigonometric extrapolation, which assumes that the fascicles are linear, ignoring the curvilinear arrangements. |
| Seymore et al., 2017<br><br>— | "Cross-sectional images were acquired along the length of the muscle at 11 equidistant points from the most distal cross-sectional image of the muscle that could be traced and measured, which is just proximal to the musculotendinous junction, to the gluteal fold; encompassing 0–100% of the visualized muscle length. Two images for each of the 11 cross-sectional points were recorded. Two longitudinal images were then recorded to allow for the estimation of fascicle length and pennation angle." | Not reported the methodology used (linear-EFOV or non-linear EFOV).<br><br>Not reported the localization of the ROI site, in relation to the bone or muscle.<br><br>Not indicate the path and orientation of the probe. |

| Study& Method | General Procedures | Methodological considerations |
|---|---|---|
| Tosovic et al., 2016<br><br>**LINEAR EFOV /STATIC** | ".. along with the most proximal and distal extents of muscle fiber insertion onto the proximal and distal tendons respectively, were scanned and the position of each was marked on the skin. Using these skin markings the following lengths were recorded with a flexible tape measure."<br><br>"Additional scans were taken systematically, at four points along BFlh, namely at 30, 50, 70, and 90% of the total muscle length."<br><br>"Still ultrasound images were also taken with the probe aligned along the long axis of BFlh, and these images were imported as DICOM files into ImageJ (National<br><br>Institutes of Health, Bethesda, MD) for analysis of FL and FA (undertaken by DT) (Fig. 1B).<br><br>Fascicle length was defined as the length of an entire muscle fascicle that extended from the superficial aponeurosis to the deep intramuscular aponeurosis and was calculated by setting the appropriate scale and using the "straight line tool" in imageJ software." | In the linear method, assumes a linear orientation for the FL, but the FL are curve.<br><br>In the static method, estimated the fascicle length using trigonometric extrapolation, which assumes that the fascicles are linear, ignoring the curvilinear arrangements.<br>Same placement of the probe for all the subjects. |

| Study& Method | General Procedures | Methodological considerations |
|---|---|---|
| Bennett et al., 2014<br><br>**NON-LINEAR EFOV** | "First, the full length of the muscle was measured twice on each image using digital calipers, starting at the most proximal point of the muscle before the musculotendinous junction, and ending at the most distal point of the muscle."<br>"Two fascicles were measured in each region of the BFlh, starting at the fascicle's superficial origin and ending at the fascicle's insertion onto the deep aponeurotic tendon."<br><br>"As the transducer was removed between contractions, measured fascicles are likely not the same fascicles, but are within a specified region of fascicles." | Only perform 2 sonograms along the total length of the muscle and trace in the sonogram a line at 50% for the total length of the field of view.<br><br>Do not guarantee that analyse the same fascicles in the two scans.<br><br>Not reported the path and orientation of the probe and if the orientation is according to the FL. |
| Gonçalves et al., 2017<br><br>**NON-LINEAR EFOV** | "Three regions of the muscle were defined using as a reference the shadow of the reflective tape and 4 fascicles for each region were digitized in the image (FIGURE 3). Only distal and middle regions of the muscle were used due to the poor quality of the images. The line was digitized from the superficial aponeurosis and the fascicles were followed until the deep aponeurosis.<br>In case of having images with curved fascicles, they were tracked in a series of connected lines." | Not report which % was the ROI in relation to the muscle length.<br>Not follow the orientation of the fascicles.<br><br>Reported that the use of EFOV ultrasound technique shows to be highly reliable to measure FL but poor to measure PA and MT. Affirmed that is a valid method to measure directly FL of the BF in future research.<br><br>Reported poor quality of the images. |

**Legend:** Fascicle length (FL); Fascicle angle (FA); Muscle Thickness (MT); Bicep femoris long head (BFlh); Vastus lateralis (VL); Ultrasound (US); Region of interest (ROI).

*Probe Position*

Regarding the probe positioning used in the previous studies (Table 1), different anatomical criteria have been used to identify the BFlh region of

interest, including (i) the mid-distance (i.e. 50%) between the ischial tuberosity and the knee joint fold (Alonso-Fernandez et al., 2017; Timmins, Bourne, et al., 2016; Timmins, Shield, Williams, Lorenzen, & Opar, 2015), (ii) between the greater trochanter and head of the fibula (Oliveira et al., 2016b), (iii) between the greater trochanter and the lateral knee joint line (Blackburn et al., 2014), and (iv) between the greater trochanter and the tibial condyle (Potier, Alexander, & Seynnes, 2009). Additionally, studies have used different percentages of the distance between the anatomical landmarks, such as 33% (Cepeda et al., 2015), or 10%, 30%, 50% and 70% (Kellis, Galanis, Natsis, & Kapetanos, 2009). Previous research performed using human cadavers has shown that the distal region of BFlh presents shorter fascicles compared to the proximal region (Kellis, Galanis, Kapetanos, & Natsis, 2012). This indicates that measurements have been performed at different percentages of muscle length, which will partly explain the fascicle length differences found between studies.

*Probe width*

Regarding the probe data collection, the majority of previous studies used a probe with a width varied between 4 and 5-cm (Alonso-Fernandez et al., 2017; Ribeiro-Alvares, Marques, Vaz, & Baroni, 2018; Cepeda, Lodovico, Fowler, & Rodacki, 2015; Potier, Alexander, & Seynnes, 2009; Timmins, Bourne, et al., 2016; Timmins, Shield, Williams, Lorenzen, & Opar, 2015). Among the studies using a probe width between 6 to 8-cm (G. S. Chleboun, France, Crill, Braddock, & Howell, 2001; e Lima et al., 2015; Freitas, Marmeleira, Valamatos, Blazevich, & Mil-Homens, 2017; Freitas & Mil-Homens, 2015b; Kellis, 2016), only Freitas et al. (2017) reported acceptable reproducibility (Freitas et al., 2017).

# CHAPTER III

# METHODS

# CHAPTER III – METHODS

*Type of study*

A test-retest study design was implemented to achieve the purpose of the study.

*Participants*

Twenty male physically active adults (age: 24.4 ± 5.7 years; height: 175 ± 0.8 cm; body mass: 73 ± 9.0 kg) without history of hamstring strain injury were invited to participate in this study. The sample size was estimated by use of G*Power software for the one-way repeated measures analysis of variance test, considering an effect size of 0.4, significance level of 0.05, statistical power of 0.8, and a correlation factor of 0.8 (for the primary outcome variable of fascicle length). For convenience, only men were recruited as they present less subcutaneous and intramuscular adipose tissue in the thigh than women, which allowed for greater sonogram echogenicity and thus muscle fascicle identification. The recruitment process was implemented by spreading word of mouth locally in the university environment and at health clubs and using social networks. All participants read and signed an informed consent document before participation in the study. No compensation and/or reimbursement for participation in the study was given. The Ethics Committee of the Faculty of Human Kinetics (University of Lisbon) approved the study (approval number: 1/2018).

*Protocol*

Participants were invited to visit the laboratory on two occasions on the same day, with 1 hour of rest between sessions. Note that during this time, other

participants were analyzed to ensure that the examiner did not memorize the orientation and path of the probe for each individual. In both sessions, the participant was positioned in ventral decubitus with the knees fully extended and asked to completely relax during the sonographic scans. The locations of the proximal and distal myotendinous junctions (MTJ) were identified using ultrasound scanning and then marked on the skin, and the distance between these two points was considered as representative of BFlh muscle length. The region of interest (ROI) where the BFlh architecture was assessed, was identified in the first session, according to the procedures described previously (Sandro R. Freitas et al., 2017). Briefly, the ROI corresponded to the site within the BFlh belly where both superficial and mid-belly aponeuroses were parallel (as best as possible), the muscle thickness (i.e. perpendicular distance between superficial and mid-belly aponeurosis) were greatest, and the hyperechoic lines delineating the BFlh fascicles (i.e. perimysial membranes) were well visualized for the maximum of their lengths. To find this ROI, both longitudinal and transverse scans were performed. A line was then drawn on the skin surface corresponding to the midpoint of the ROI so that repeated measures could always be performed at the same site. To ensure that the ultrasound transducer was correctly aligned with the ROI among the repeated measurements, a marker corresponding to the midpoint of the sonogram field of view was drawn on both sides of the transducer. The distance from the distal myotendinous junction to the ROI was measured so the sonographic measurements could be repeated in the second session. According to a previous study (14) this site corresponds to approximately 55% of (distal to proximal) BFlh length. After determining the ROI, three scans were performed for each sonographic technique, with the techniques implemented in a random order. At the end of the first session, all markers drawn on the skin were erased. In the second session, in order to identify the same location where the ultrasound scanning was performed in the first session, the distance between the distal

myotendinous junction and the ROI identified in the first session was used. Then scanning was performed using identical procedures to the first session.
In addition, in order to compare this ROI location to the sites used in other studies (with other anatomical criteria), the correspondence to the percent femur length between the mid-distance of (i) great trochanter to femur lateral condyle, (ii) ischial tuberosity to the knee fold, (iii) great trochanter to the knee fold, (iv) great trochanter and fibula head, and (v) gluteal fold and knee fold, was also randomly determined in nine individuals from the sample, in the first session.

*Muscle architecture assessment*

An ultrasound scanner (EUB-7500; Hitachi Medical Corporation, Chiyoda-ku, Tokyo, Japan), coupled with a 6-cm linear probe operating at a 10 MHz frequency was used to assess BFlh architecture using three distinct techniques in B mode. During data acquisition for all techniques, minimal pressure was applied to the skin. Hidrogel was used to improve acoustic contact between the probe and skin, and therefore improve image quality. For the EFOV imaging, a sampling frequency of 47Hz was used.

*Sonographic technique descriptions*

Three sonographic techniques were used to assess BFlh architecture: i) static-image; ii) linear-EFOV; and iii) nonlinear-EFOV. Figure 6 shows an example of a sonogram captured using each technique.

For the static-image technique, sonograms were acquired at the site where the ROI was central within the sonogram field of view and orientating the ultrasound probe according to the fascicles direction. In order to identify the ROI center in the EFOV sonograms, a wire was placed at the ROI center during

the acquisition. This allowed to align the sonograms taken by the different techniques in respect to the ROI center. For the linear-EFOV technique, the ultrasound transducer was initially centered with the ROI and orientated according to the fascicle direction at that point in the muscle. Because the location within the probe length that constructs the EFOV sonograms was 0.6 cm proximally from the center of the probe (with a ~1.2 cm field of view width), the probe was then moved ~2.4 cm proximally with the probe orientation remaining consistent to start the image acquisition. Note that this was performed in order to guarantee the same visualization of the fascicles as observed in the static images. A slow and constant transducer motion was performed following a linear path with the help of a plastic guide, according to the orientation of the fascicles visualized at the image acquisition start. For the nonlinear-EFOV technique the direction of the ultrasound probe was altered (approximately every ~1 cm) during acquisition according to fascicle direction. To accomplish this, the fascicle orientation at the ROI was first determined and the probe orientation marked. The probe was then moved along the fascicle path identified by extensive visualization of the path prior to data collection; both the fascicular path and optimal probe orientation were determined, and practice scans were completed before the data collection scans. At the start of image acquisition, the probe was moved ~2.4-cm proximal to the ROI site (similar to the linear-EFOV technique) and a nonlinear path was then followed.

*Data processing*

All sonograms were digitized using ImageJ software (NIH, 1.47v, USA), and fascicle length, fascicle angle, and muscle thickness were determined from each sonogram. As only part of fascicle could be visualized during static-image

assessments, the linear extrapolation method was used to estimate the non-visible fascicle part (Noorkoiv et al., 2010), using the following equation (2):

$$FL=L+(h/\sin\beta) \quad (2)$$

where *L* is the observable fascicle length from the mid-muscle aponeurosis to the most visible end-point, *h* is the perpendicular distance between the superficial aponeurosis and the fascicle's visible distal end-point, and $\beta$ is the angle between the fascicle (drawn linearly to the most distal point) and the superficial aponeurosis. Muscle thickness was measured as the distance between the superficial and the mid-muscle aponeurosis measured at ROI site.

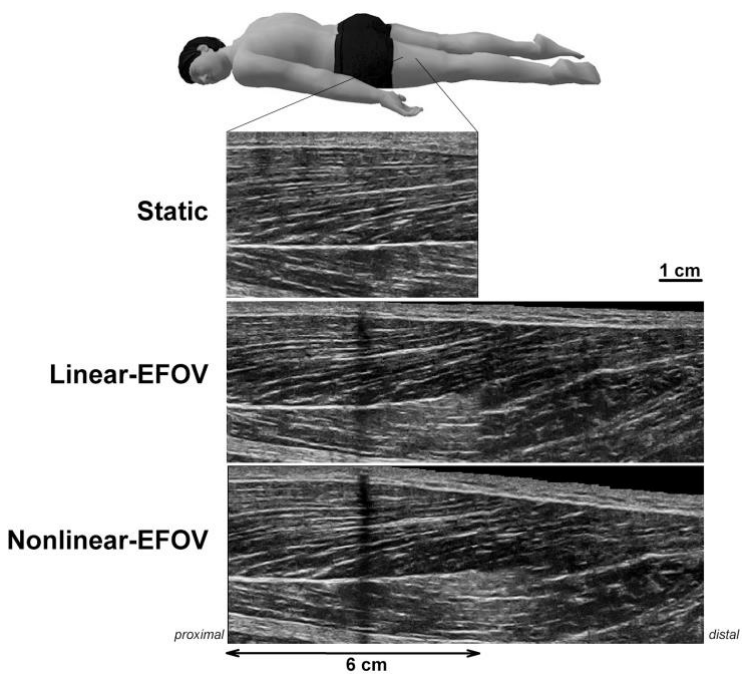


**Figure 6**. Sonograms of biceps femoris long head from one individual (#13) assessed at a given region of interest using the three techniques: static-image, linear-EFOV, and nonlinear-EFOV.

For EFOV images, fascicle length was determined from the mid-aponeurosis origin to the superficial aponeurosis insertion of the fascicles. For static-image and linear-EFOV images the fascicle length was determined using the straight-line drawing tool in the ImageJ software, while for the nonlinear-EFOV images the fascicle was tracked using the segmented line tool. In each sonogram, the average length and angle of three fascicles inserting onto the mid-belly aponeurosis within 3 cm proximal to the ROI center was used as a representative measure for that image. The average from the three consecutive images for each sonographic technique was determined and used for statistical analysis. The researcher was blinded to the sonograms measurement during the digitization process.

*Statistical analysis*

The statistical analysis was completed by a researcher blinded to the participants' identities using SPSS software (v20, Chicago,USA). One-way repeated measures analysis of variance was performed followed by post-hoc analysis (Bonferroni test) to test for differences between the percentage distance along the femur at which the ROI was situated in the current analysis and those published by other researchers. The test-retest repeatability for each technique was determined by calculating the intraclass correlation coefficient ($ICC_{3,k}$), Pearson's correlation coefficient (r), and standard error of measurement (SEM) (Hopkins, 2000). A paired t-test was performed to determine whether the measurements differed between sessions. Intra-day repeatabilities were classified as little (ICC<0.25), low (0.26–0.49), moderate (0.50–0.69), high (0.70–0.89), and very high (>0.90) (Domholdt, 1993).

Normality of data was confirmed using the Shapiro-Wilk test. One-way repeated measures analysis of variance was performed for fascicle length, fascicle angle, and muscle thickness to determine whether differences existed between the sonographic techniques (static-image vs. linear-EFOV vs. nonlinear-EFOV). Post-hoc analysis was performed using Bonferroni tests. Cohen's effect size (*d*) was calculated to provide clinical meaningfulness of the differences. Significance was set at 0.05. The magnitudes of *d* were classified as trivial (<0.20), small (0.21 –0.60), moderate (0.61 –1.20), large (1.21 –2.00), very large (2.01 –4.00) and extremely large (>4.00) (S. R. Freitas et al., 2018). Considering the nonlinear-EFOV technique as the gold standard, we additionally determined the absolute mean error of the static-image and linear-EFOV techniques by calculating the difference between the measurements.

The measurement of agreement between the sonographic techniques was examined using Bland-Altman analysis (Giavarina, 2015), and the Spearman's rank-order correlation coefficient (*rho*) was computed in order to determine if the individuals would have a similar rank within the sample when using the different sonographic techniques (i.e. whether conclusions regarding the rank of a participant within the cohort vary between techniques). The magnitudes of both Spearman's and Pearson's coefficients were classified as weak (< 0.3), moderate (0.3-0.7) and strong (>0.7) (Sheskin, 2000).

# CHAPTER IV

# **RESULTS**

# CHAPTER IV – RESULTS

Participants had femur and BFlh lengths of 42.2 ± 2.7 cm and 30.3 ± 1.7 cm, respectively. The ultrasound probe was therefore positioned 21.9 ± 2.8 cm from the lateral femoral condyle (i.e. 52.0 ± 5.0% of femur length) and 17.2 ± 2.1 cm from the distal myotendinous junction (i.e. 57.0 ± 6.0% of BFlh length). The ultrasound probe placement with respect to the femur length was not statistically different from the mid-distance (i.e. 50%) of femur length ($p=0.125$), ischial tuberosity to the knee fold (50±1% of femur length; $p=1.0$), the greater trochanter to the knee fold (54±5%; $p=1.0$), or greater trochanter to the fibula head (47±1%; $p=0.155$); however it was different from the mid-distance between the gluteal fold and knee fold (29±4%; $p<0.001$).

Table 2 shows the repeatability outcomes for the assessment of BFlh architecture parameters using the three different sonographic techniques. For fascicle length, very high repeatability was found for both the static-image and nonlinear-EFOV techniques, while a high repeatability was observed for the linear-EFOV technique. For fascicle angle and muscle thickness, a high repeatability was observed for both static-image, linear-EFOV and nonlinear-EFOV techniques. Trivial differences (i.e. $d<0.16$) were noted between the measurements for all BFlh architecture variables.

**Table 2.** Intra-day repeatability outcomes for the assessment of biceps femoris (long head) fascicle length, fascicle angle, and thickness using three different sonographic techniques: static-image, linear-EFOV, and nonlinear-EFOV.

**Note:** (i) measure 1 and 2 refers to the sessions 1 and 2, respectively; and, (ii) the p-value, as well the Cohen´s d effect size, refers to the differences between measures 1 and 2.

| Outcome | Technique | Measure 1 | Measure 2 | $ICC_{3,k}$ [95%CI] | r | SEM (mm) | p-value | *d* |
|---|---|---|---|---|---|---|---|---|
| **Fascicle length (mm)** | Static-image | 84.1 ± 12.3 | 85.8 ± 11.7 | 0.92 [0.81-0.97] | 0.93 | 3.2 | 0.112 | 0.14 |
| | Linear-EFOV | 75.1 ± 8.1 | 76.2 ± 8.5 | 0.86 [0.68-0.94] | 0.86 | 3.1 | 0.263 | 0.13 |
| | Nonlinear-EFOV | 76.9 ± 8.7 | 78.1 ± 9.1 | 0.95 [0.86-0.98] | 0.95 | 1.9 | 0.065 | 0.13 |
| **Fascicle angle (º)** | Static-image | 16.4 ± 2.9 | 16.6 ± 2.6 | 0.86 [0.68-0.94] | 0.86 | 1.1 | 0.563 | 0.07 |
| | Linear-EFOV | 18.1 ± 3.0 | 18.2 ± 3.1 | 0.87 [0.69-0.95] | 0.86 | 1.1 | 0.700 | 0.03 |
| | Nonlinear-EFOV | 18.0 ± 4.7 | 18.1 ± 4.2 | 0.97 [0.92-0.99] | 0.97 | 0.8 | 0.719 | 0.02 |
| **Muscle thickness (mm)** | Static-image | 24.1 ± 2.0 | 24.4 ± 2.1 | 0.94 [0.85- 0.98] | 0.95 | 0.5 | 0.062 | 0.15 |
| | Linear-EFOV | 23.9 ± 1.9 | 24.0 ± 2.1 | 0.93 [0.84 -0.97] | 0.94 | 0.5 | 0.706 | 0.05 |
| | Nonlinear-EFOV | 24.1 ± 2.0 | 24.3 ± 2.2 | 0.96 [0.89-0.98] | 0.96 | 0.4 | 0.172 | 0.10 |

**Legend**: ICC, intraclass correlation coefficient; r, pearson's coefficient; SEM, standard error of the mean; p-value, obtained from a paired t-test; *d*, Cohen's effect size.

Figure 7 shows the differences between the sonographic techniques for the various BFlh architecture outcomes. A greater fascicle length was estimated when using the static-image technique than the linear-EFOV (moderate effect, $d$=0.92; p<0.001) and nonlinear-EFOV (moderate effect, $d$=0.71; p<0.001) techniques, but a smaller fascicle angle was observed compared to the linear-EFOV (small effect, $d$=0.59; p=0.001) and nonlinear-EFOV (small effect, $d$=0.42; p=0.112) techniques. No differences were detected between the techniques for muscle thickness (p>0.191). Using the static-image sonographic

technique, 35.4 ± 7.0% of the fascicle length was estimated using the linear extrapolation technique, with the remainder length measured in the visible sonogram.

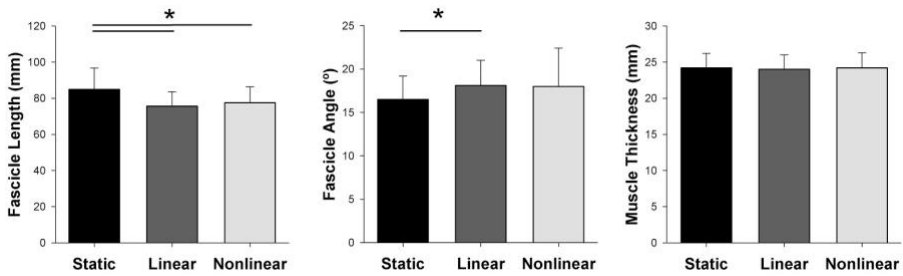


**Figure 7**. Fascicle length, fascicle angle, and muscle thickness of biceps femoris (long head) assessed using static-image (static), linear-EFOV (linear), and nonlinear-EFOV (nonlinear) techniques.
* Significant differences between the sonographic techniques ($P<0.05$).

The linear regression (A) and the Bland & Altman analysis plots (B and C for absolute and relative values, respectively) for fascicle length and angle are presented in Figures 8 and 9 respectively. An acceptable linearity was observed between the sonographic techniques for both fascicle length (Figure 8-A) and fascicle angle (Figure 9-A). For fascicle length, the static-image technique appeared to overestimate the measurement when compared to both the linear-EFOV and nonlinear-EFOV techniques (Figure 8-B and C). For fascicle angle, the static-image technique underestimated the measurement when compared to the linear-EFOV and nonlinear-EFOV techniques (Figure 9-B and C). When compared to the nonlinear-EFOV technique, the average absolute error was 7.9±6.1 mm (static-image) and 3.7±3.0 mm (linear-EFOV) for the fascicle length; and 1.9±2.9º (static-image) and 1.8±2.9º (linear-EFOV) for the fascicle angle.

When comparing the static-image to the linear-EFOV technique, a moderate correlation was found between the measurement difference (in both absolute and relative values) and the average measurement for the fascicle length (see static-image vs. linear-EFOV in Figure 8 B-C), but this was not the case for the fascicle angle (Figure 9 B-C). When comparing the static-image to the nonlinear-EFOV technique, a moderate association was found between the absolute measurement difference (but not for the relative values) and the average measurement for the fascicle length (see static-image vs. linear-EFOV in Figure 8 B-C), but this was not the case for fascicle angle (Figure 9 B-C). No association was found between the measurement difference and the average measurement when comparing the linear-EFOV to the nonlinear-EFOV technique in both fascicle length (Figure 8) or fascicle angle (Figure 9) outcomes.

A strong Spearman's coefficient was found between sonographic techniques for both the fascicle length (i.e. static-image vs. linear-EFOV: *rho*=0.86, $p<0.001$; static-image vs. nonlinear-EFOV: *rho*=0.81, $p<0.001$; linear-EFOV vs. nonlinear-EFOV: *rho*=0.89, $p< 0.001$) and fascicle angle (i.e. static-image vs. linear-EFOV: *rho*=0.83, $p<0.001$; static-image vs. nonlinear-EFOV: *rho*=0.81, $p<0.001$; linear-EFOV vs. nonlinear-EFOV: *rho*=0.86, $p< 0.001$) measurements, indicating that the ranking of participants on these outcomes within the cohort was similar, although not perfectly the same (please see supplementary data). Nevertheless, individuals' rankings within the cohort differed on average 2.9 and 2.3 places for the fascicle length when determined by the static-image and linear-EFOV, respectively, compared to nonlinear-EFOV.

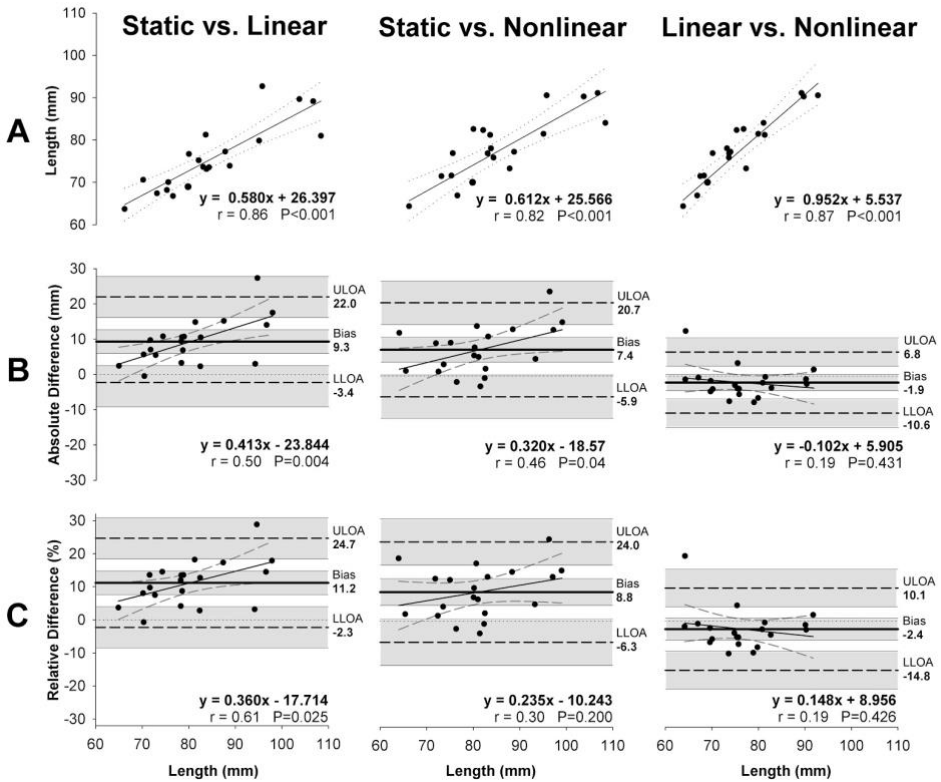


**Figure 8**. Agreement of fascicle length measurements between the three sonographic techniques: Linear regression analysis (A), and Bland & Altman analysis with (B) absolute and (C) relative differences (i.e. differences between the techniques normalized to average value between the techniques) with respect to the average fascicle length obtained between the techniques (x-axis of B and C graphs).

Legend: ULOA, upper limit of agreement; LLOA, lower limit of agreement.
Note: The first method presented in each title at the top corresponds to the values shown on the y-axis of the linear regression plot.

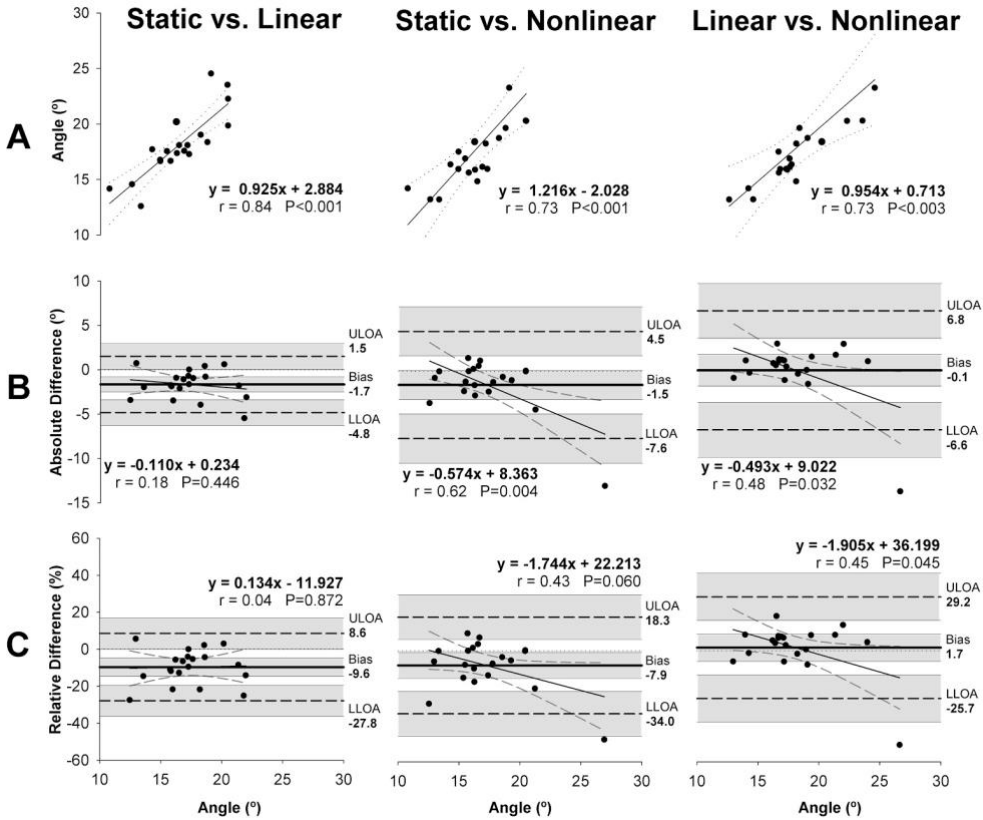


**Figure 9**. Agreement of fascicle angle measurements between three sonographic techniques: Linear regression analysis (A), and Bland & Altman analysis with (B) absolute and (C) relative differences (i.e. differences between the techniques normalized to average value between the techniques) with respect to the average fascicle angle obtained between the techniques (x-axis of B and C graphs).

Legend: ULOA, upper limit of agreement; LLOA, lower limit of agreement.
Note: The first method presented in each title at the top corresponds to the values shown on the y-axis of the linear regression plot.

# CHAPTER V

# DISCUSSION

# CHAPTER V – DISCUSSION

To our knowledge, this is the first study to compare the repeatability of, and measurement agreement between, different sonographic techniques used to assess BFlh architecture outcomes. The main findings were: i) the three sonographic techniques showed acceptable repeatability, with the nonlinear-EFOV technique showing the highest repeatability overall; ii) the fascicle lengths measured using the static-image technique were longer, and fascicle angles smaller, compared to both linear-EFOV and nonlinear-EFOV sonographic techniques; and iii) despite strong Spearman's correlations being observed, the rank order of participants (based on their fascicle length) differed between techniques, so conclusions made regarding their relative (to a cohort) length, and therefore conclusions relating to muscle contractile properties that are influenced by fascicle length, will differ based on the technique used.

An important finding was that the test repeatabilities observed in the present study were acceptable regardless of the sonographic technique used (i.e. ICC>0.86), and similar to those reported previously (Bennett et al., 2014; Chleboun et al., 2001; Sandro R. Freitas et al., 2017; Oliveira et al., 2016; Potier, Alexander, & Seynnes, 2009; Sá et al., 2016; Seymore et al., 2017b; Timmins, Shield, Williams, Lorenzen, & Opar, 2015; Tosovic et al., 2016). However, and contrary to our initial expectation, a greater repeatability of outcomes was observed for the nonlinear-EFOV technique. Importantly, very high repeatability was noted for the nonlinear-EFOV technique in all outcomes, but this was not the case for the linear-EFOV (i.e. in both fascicle length and angle) or static-image (i.e. for fascicle angle only) techniques. We contend that this difference can be explained in two ways. First, because the linear-EFOV technique was performed using the same probe orientation along its measurement plane, the hyperechoic regions (which are assumed to represent the perimysium fractions of the muscle fascicles and interfascicular

adipose tissue and blood vessels) in the distal region of the sonograms were of poorer resolution. Consequently, the difficulty inherent in digitizing the fascicle end points in the distal regions was increased. Note that this did not occur when using the nonlinear-EFOV technique because the probe orientation was changed according to fascicle orientations along their path. The second reason relates to the digitization procedure, which was different between techniques. While in the static-image and linear-EFOV techniques a *straight line* tool was used digitize the fascicle point of interest in the static-image and linear-EFOV measurements, the *segmented line* tool was used for the nonlinear-EFOV technique. Therefore, being able to image more of the fascicle, as was the case using the linear-EFOV technique, did not improve repeatability estimates sufficiently to match the more complex, but more reliable, nonlinear-EFOV technique.

It is important to note that some muscles present fascicles with a curve path at rest (Blazevich, Cannavan, Coleman, & Horne, 2007), although the curvatures may be changed by either passive stretch (Bolsterlee, D'Souza, Gandevia, & Herbert, 2017) or active contraction (Otten, 1988). In our study, we asked the individuals to fully relax, and noted (by visualizing the sonograms) that fascicles assumed a nonlinear path; in fact, in a number of cases a double curvature was noted where concave gave way to convex fascicle curvature (e.g. Figure 6, the nonlinear-EFOV sonogram at bottom). As the *segmented line* tool allows the researcher to follow the fascicle paths more accurately, whereas the *straight line* tool only allows digitization of two points within the sonogram, we assume that small differences in repeatability may be related to this, and that the measurement error (i.e. compared to the theoretically-correct nonlinear-EFOV technique; see Figure 7) was increased with the curvature of the fascicles.

It is also noteworthy that the BFlh architecture outcomes reported in the present study were somewhat different from those reported in previous studies. In general, a shorter fascicle length and higher fascicle angle was observed for the static-image technique in the present study, despite similar muscle thickness values being found. Although architectural parameters vary considerably between individuals, and thus average architectural parameters will differ between studies, we suggest that differences in the data collection and digitatizion processes are important.

Regarding the data collection, a wider ultrasound probe (i.e. 6 cm) was used in the present study whilst the majority of previous studies have used probe widths of 4 to 5 cm (Alonso-Fernandez, Docampo-Blanco, & Martinez-Fernandez, 2017; Cepeda, Lodovico, Fowler, & Rodacki, 2015; Potier et al., 2009; Ribeiro-Alvares et al., 2018; Timmins et al., 2016, 2015). In the present study, using a 6-cm probe for the static-image technique, on average 35.4±7.0% of the fascicle length was estimated using a linear extrapolation technique because the fascicles were extended off the field of view. Given the smaller probe width used in previous studies, a greater proportion of the fascicle length would need to have been estimated (e.g. ~70% in Timmins et al., 2016). Interestingly, we found that fascicle length was overestimated when using the static-image technique as compared to the EFOV techniques, and such overestimation was greater for longer fascicles (except for relative values between static-image and nonlinear-EFOV techniques, see Fig. 8 B-C); note that this was not the case for fascicle angle. Assuming that the extent of overestimation is positively and linearly associated to the probe width, each 1-cm probe width reduction would correspond to an additional ~11% overestimation of fascicle length. Given the linear and positive relationship (r=0.46-0.61) between the extent of fascicle length overestimation when using the static-image technique compared to the EFOV techniques and assuming

the fascicle lengths reported herein are accurate (i.e. for an average fascicle length of 84 mm there was 8-11% of overestimation, Fig. 8 B-C), we contend that previous studies using a probe width of 4.5 cm have may overestimated fascicle length by at least 25%. This explains why previous data captured using sonogram probe widths of 4 to 5 cm have reported larger fascicle lengths than in the current study (Blackburn, Troy Blackburn, & Pamukoff, 2014; Cepeda et al., 2015; Ribeiro-Alvares et al., 2018; Timmins et al., 2016, 2015). For instance, Ribeiro-Alvares et. al (2018) used a 4-cm probe width and reported longer fascicles (i.e. 94 mm) despite finding lower values for muscle thickness (i.e. 21 mm), although their subjects also seemed to have smaller fascicle angles (i.e. 12.8º). This suggests that more than 57% of the FL was estimated using linear extrapolation technique, which may be problematic from a perspective of obtaining accurate estimates of FL. Future research is required to compare the degree of overestimation when using different ultrasound sonogram widths.

Another important finding of the present study was that the Spearman's coefficients between techniques were strong but imperfect for both fascicle length and angle. This indicates that the ranking of participants on these outcomes within the cohort must be dissimilar. For example, on average each participant was ranked 2.9 places different (in the cohort of 20) between the static-image and nonlinear-EFOV techniques, which is a mean shift in position within the group of 14.5% (please see supplementary data). The maximum difference in ranking between these techniques was 8 (i.e. ranked 8$^{th}$ by static-image and 16$^{th}$ by nonlinear-EFOV), which suggests that conclusions relating to muscle function and injury risk based on the fascicle length would be very different between techniques for this individual. Such findings prompt the consideration of previous results (both experimental, retrospective, and prospective studies) assessing BFlh architecture. For instance, BFlh fascicle

length has been suggested to be an important diagnostic tool for estimating hamstring strain injury risk (Timmins et al., 2016, 2015). Considering that a change in the rank of someone within a sample would change their diagnosis, it is reasonable that confidence may be reduced when using such techniques. Future studies should determine whether similar conclusions are obtained when assessing BFlh architecture using the nonlinear-EFOV technique.

Regarding the location of imaging within the muscle, the region of interest used to examine BFlh architecture has varied substantially between previous studies. Different anatomical criteria have been used to identify the BFlh region of interest, including (i) the mid-distance (i.e. 50%) between the ischial tuberosity and the knee joint fold (Alonso-Fernandez et al., 2017; Timmins et al., 2016, 2015), (ii) between the greater trochanter and head of the fibula (Oliveira et al., 2016), (iii) between the greater trochanter and the lateral knee joint line (Blackburn et al., 2014), and (iv) between the greater trochanter and the tibial condyle (Potier et al., 2009). Additionally, studies have used different percentages of the distance between the anatomical landmarks, such as 33% (Cepeda et al., 2015), or 10%, 30%, 50% and 70% (Kellis et al., 2009). As shown in the present study, the different anatomical landmarks produced a different location (either proximal or distal) compared to the site determined using our criteria. This means that previous observations were performed at different regions within the muscle. Research on human cadavers has shown that the distal region of BFlh presents shorter fascicles compared to the proximal region (Kellis, Galanis, Kapetanos, & Natsis, 2012). This indicates that measurements have been performed at different percentages of muscle length, which will partly explain the fascicle length differences found between studies. The procedure used in the present study was similar to that published previously (Sandro R. Freitas et al., 2017), where the BFlh fascicles could be well visualized, capturing both the superficial and mid-muscle aponeuroses as

parallel as possible. The comparison of architecture at different BFlh lengths should be examined in future research.

It is important to note some methodological considerations when interpreting the results of the present study. First, in order to make use of the smaller subcutaneous adipose thickness and greater echogenicity of the fascicle boundaries (Sandro R. Freitas et al., 2017), only men were examined in the present study. Nonetheless, we assume that findings would have been similar if women were included in the study. Second, BFlh myoelectric activity was not assessed during the measurements; since fascicle curvature changes with activation, it is possible for small muscle contractions to affect measurements. Although muscle activity might be monitored in future studies, the participants were asked to remain fully relaxed during assessments, and we believe it is unlikely that muscles were contracted during data collection. Third, it is reasonable to hypothesize that a different ultrasound probe location in the transverse plane was used between the techniques; this is particularly the case for the nonlinear-EFOV technique, since it assumes a nonlinear path during the scanning. However, no differences in the muscle thickness at the ROI were seen between the techniques, which suggests that this (potential) misalignment was minimal. Finally, previous studies have reported that fascicle angle may be underestimated by ultrasound measurement when compared to diffusion tensor magnetic resonance imaging (Bolsterlee, Veeger, van der Helm, Gandevia, & Herbert, 2015), possibly due to the probe pressure on the skin during image capture. As fascicle angle is used to estimate fascicle length in the static-image technique, small errors in fascicle angle will subsequently affect fascicle length estimation. We paid close attention to the minimization of probe pressure during the performance of all techniques, and therefore assume that the conclusions of this study are not notably affected.

# CHAPTER VI

# CONCLUSION

# CHAPTER VI – CONCLUSION

We found an acceptable repeatability when assessing biceps femoris long head fascicle length and angle at a given region of interest when using three different sonographic techniques, although the nonlinear-EFOV technique showed the highest repeatability. Nonetheless, we found that the static-image technique overestimated fascicle length and underestimated the fascicle angle when compared to both the nonlinear-EFOV and linear-EFOV techniques. This difference may be explained by the smaller field of view allowed by the static-image technique (evidenced by differences between static-image and linear-EFOV methods, where a straight line of the fascicles was assumed) but also may be explained partly by the way fascicle curvature is accounted for (or not, with the static-image and linear-EFOV techniques). Furthermore, the ranking of participants within the cohort was altered appreciably (by 2.9 places on average, with maximum of 8 places in the sample of 20 participants) when measurements were performed using the nonlinear-EFOV technique compared to the static-image technique. Researchers and practitioners should therefore consider that BFlh fascicles present significant curvature, that this curvature may change along the muscle's length, and that this complexity may affect conclusions derived from research that adopts different sonographic methods. Researchers examining biceps femoris long head architecture at a similar percentage of muscle length should, consider the present methodological findings when choosing a sonographic technique for use as well as when interpreting the results of other research studies.

## REFERENCES


Aagaard, P., Andersen, J. L., Dyhre-Poulsen, P., Leffers, A.-M., Wagner, A., Peter Magnusson, S., Simonsen, E. B. (2001). A mechanism for increased contractile strength of human pennate muscle in response to strength training: changes in muscle architecture. *The Journal of Physiology*, *534*(2), 613–623.

Abe, T., Kumagai, K., & Brechue, W. F. (2000). Fascicle length of leg muscles is greater in sprinters than distance runners. *Medicine and Science in Sports and Exercise*, *32*(6), 1125–1129.

Akagi, R., Takai, Y., Ohta, M., Kanehisa, H., Fukunaga, T., & Kawakami, Y. (2011). Size–strength relationships of the elbow flexors and extensors are not affected by age or gender. *European Journal of Sport Science: EJSS: Official Journal of the European College of Sport Science*, *11*(4), 277–282.

Akagi, R., Takai, Y., Ohta, M., Kanehisa, H., Kawakami, Y., & Fukunaga, T. (2009). Muscle volume compared to cross-sectional area is more appropriate for evaluating muscle strength in young and elderly individuals. *Age and Ageing*, *38*(5), 564–569.

Alonso-Fernandez, D., Docampo-Blanco, P., & Martinez-Fernandez, J. (2017). Changes in muscle architecture of biceps femoris induced by eccentric strength training with nordic hamstring exercise. *Scandinavian Journal of Medicine & Science in Sports*.

Arnason, A., Andersen, T. E., Holme, I., Engebretsen, L., & Bahr, R. (2008). Prevention of hamstring strains in elite soccer: an intervention study. *Scandinavian Journal of Medicine & Science in Sports*, *18*(1), 40–48.

Askling, C., Karlsson, J., & Thorstensson, A. (2005). Hamstring injury occurrence in elite soccer players after preseason strength training with eccentric overload. *Scandinavian Journal of Medicine & Science in Sports*, *15*(1), 65–65.

Basser, P. J., & Jones, D. K. (2002). Diffusion-tensor MRI: theory, experimental design and data analysis - a technical review. *NMR in Biomedicine*, *15*(7-8), 456–467.

Basser, P. J., Mattiello, J., & LeBihan, D. (1994). MR diffusion tensor spectroscopy and imaging. *Biophysical Journal*, *66*(1), 259–267.

Basser, P. J., & Pierpaoli, C. (1996). Microstructural and physiological features of tissues elucidated by quantitative-diffusion-tensor MRI. *Journal of Magnetic Resonance. Series B*, *111*(3), 209–219.

Bennett, H. J., Rider, P. M., Domire, Z. J., DeVita, P., & Kulas, A. S. (2014). Heterogeneous fascicle behavior within the biceps femoris long head at different muscle activation levels. *Journal of Biomechanics*, *47*(12), 3050–3055.

Blackburn, J. T., Troy Blackburn, J., & Pamukoff, D. N. (2014). Geometric and architectural contributions to hamstring musculotendinous stiffness. *Clinical Biomechanics* , *29*(1), 105–110.

Blazevich, A. J., Cannavan, D., Coleman, D. R., & Horne, S. (2007). Influence of concentric and eccentric resistance training on architectural adaptation in human quadriceps muscles. *Journal of Applied Physiology*, *103*(5), 1565–1575.

Bolsterlee, B., D'Souza, A., Gandevia, S. C., & Herbert, R. D. (2017). How does passive lengthening change the architecture of the human medial gastrocnemius muscle? *Journal of Applied Physiology*, *122*(4), 727–738.

Bolsterlee, B., Veeger, H. E. J. D., van der Helm, F. C. T., Gandevia, S. C., & Herbert, R. D. (2015). Comparison of measurements of medial gastrocnemius architectural parameters from ultrasound and diffusion tensor images. *Journal of Biomechanics*, *48*(6), 1133–1140.

Brand, P. W., Beach, R. B., & Thompson, D. E. (1981). Relative tension and potential excursion of muscles in the forearm and hand. *The Journal of Hand Surgery*, *6*(3), 209–219.

Brockett, C. L., Morgan, D. L., & Proske, U. (2004). Predicting Hamstring Strain Injury in Elite Athletes. *Medicine & Science in Sports & Exercise*, *36*(3), 379–387.

Budzik, J. F., Le Thuc, V., Demondion, X., Morel, M., Chechin, D., & Cotten, A. (2007). In vivo MR tractography of thigh muscles using diffusion imaging: initial results. *European Radiology*, *17*(12), 3079–3085.

Burkholder, T. J., Fingado, B., Baron, S., & Lieber, R. L. (1994). Relationship between muscle fiber types and sizes and muscle architectural properties in the mouse hindlimb. *Journal of Morphology*, *221*(2), 177–190.

Cepeda, C. C. P., Lodovico, A., Fowler, N., & Rodacki, A. L. F. (2015). Effect of an Eight-Week Ballroom Dancing Program on Muscle Architecture in Older Adult Females. *Journal of Aging and Physical Activity*, *23*(4), 607–612.

Chleboun, G. S., France, A. R., Crill, M. T., Braddock, H. K., & Howell, J. N. (2001). In vivo Measurement of Fascicle Length and Pennation Angle of the Human Biceps femoris Muscle. *Cells, Tissues, Organs*, *169*(4), 401–409.

Chleboun, G. S., France, A. R., Crill, M. T., Braddock, H. K., & Howell, J. N. (2001). In vivo measurement of fascicle length and pennation angle of the human biceps femoris muscle. *Cells, Tissues, Organs*, *169*(4), 401–409.

Cleveland, G. G., Chang, D. C., Hazlewood, C. F., & Rorschach, H. E. (1976). Nuclear magnetic resonance measurement of skeletal muscle: anisotrophy of the diffusion coefficient of the intracellular water. *Biophysical Journal*, *16*(9), 1043–1053.

Close, R. (1964). DYNAMIC PROPERTIES OF FAST AND SLOW SKELETAL MUSCLES OF THE RAT DURING DEVELOPMENT. *The Journal of Physiology*, *173*, 74–95.

Connell, D. A., Schneider-Kolsky, M. E., Hoving, J. L., Malara, F., Buchbinder, R., Koulouris, G., … Bass, C. (2004). Longitudinal study comparing sonographic and MRI assessments of acute and healing hamstring injuries. *AJR. American Journal of Roentgenology*, *183*(4), 975–984.

Cooperberg, P. L., Barberie, J. (jay), Wong, T., & Fix, C. (2001). Extended field-of-view ultrasound. *Seminars in Ultrasound, CT and MRI*, *22*(1), 65–77.

Croisier, J.-L., Forthomme, B., Namurois, M.-H., Vanderthommen, M., & Crielaard, J.-M. (2002). Hamstring Muscle Strain Recurrence and Strength Performance Disorders. *The American Journal of Sports Medicine*, *30*(2), 199–203.

Damon, B. M., Ding, Z., Anderson, A. W., Freyer, A. S., & Gore, J. C. (2002). Validation of diffusion tensor MRI-based muscle fiber tracking. *Magnetic Resonance in Medicine: Official Journal of the Society of Magnetic Resonance in Medicine / Society of Magnetic Resonance in Medicine*, *48*(1), 97–104.

Denny-Brown, D. E. (1929). The Histological Features of Striped Muscle in Relation to Its Functional Activity. *Proceedings of the Royal Society B: Biological Sciences*, *104*(731), 371–411.

De Smet, A. A., & Best, T. M. (2000). MR imaging of the distribution and location of acute hamstring injuries in athletes. *AJR. American Journal of Roentgenology*, *174*(2), 393–399.

Dons, B., Bollerup, K., Bonde-Petersen, F., & Hancke, S. (1979). The effect of weight-lifting exercise related to muscle fiber composition and muscle cross-sectional area in humans. *European Journal of Applied Physiology and Occupational Physiology*, *40*(2), 95–106.

Domholdt, E. (1993). *Physical Therapy Research: Principles and Applications*. W.B. Saunders Company.

Ekstrand, J., Lee, J. C., & Healy, J. C. (2016). MRI findings and return to play in football: a prospective analysis of 255 hamstring injuries in the UEFA Elite Club Injury Study. *British Journal of Sports Medicine*, *50*(12), 738–743.

e Lima, K. M. M., E, K. M., Carneiro, S. P., de S. Alves, D., Peixinho, C. C., & de Oliveira, L. F. (2015). Assessment of Muscle Architecture of the Biceps Femoris and Vastus Lateralis by Ultrasound After a Chronic Stretching Program. *Clinical Journal of Sport Medicine: Official Journal of the Canadian Academy of Sport Medicine*, *25*(1), 55–60.

Freitas, S. R., Marmeleira, J., Valamatos, M. J., Blazevich, A., & Mil-Homens, P. (2017). Ultrasonographic Measurement of the Biceps Femoris Long-Head Muscle Architecture. *Journal of Ultrasound in Medicine: Official Journal of the American Institute of Ultrasound in Medicine*.

Freitas, S. R., & Mil-Homens, P. (2015). Effect of 8-week high-intensity stretching training on biceps femoris architecture. *Journal of Strength and Conditioning Research / National Strength & Conditioning Association*, *29*(6), 1737–1740.

Friederich, J. A., & Brand, R. A. (1990). Muscle fiber architecture in the human lower limb. *Journal of Biomechanics*, *23*(1), 91–95.

Froeling, M., Oudeman, J., Strijkers, G. J., Maas, M., Drost, M. R., Nicolay, K., & Nederveen, A. J. (2015). Muscle changes detected with diffusion-tensor imaging after long-distance running. *Radiology*, *274*(2), 548–562.

Fukunaga, T., Ichinose, Y., Ito, M., Kawakami, Y., & Fukashiro, S. (1997). Determination of fascicle length and pennation in a contracting human muscle in vivo. *Journal of Applied Physiology*, *82*(1), 354–358.

Fukunaga, T., Kawakami, Y., Kuno, S., Funato, K., & Fukashiro, S. (1997). Muscle architecture and function in humans. *Journal of Biomechanics*, *30*(5), 457–463.

Galbán, C. J., Maderwald, S., Uffmann, K., de Greiff, A., & Ladd, M. E. (2004). Diffusive sensitivity to muscle architecture: a magnetic resonance diffusion tensor imaging study of the human calf. *European Journal of Applied Physiology*, *93*(3), 253–262.

Gans, C. (1982). Fiber architecture and muscle function. *Exercise and Sport Sciences Reviews*, *10*, 160–207.

Gans, C., & de Vree, F. (1987). Functional bases of fiber length and angulation in muscle. *Journal of Morphology*, *192*(1), 63–85.

Gans, C., & Gaunt, A. S. (1991). Muscle architecture in relation to function. *Journal of Biomechanics*, *24 Suppl 1*, 53–65.

Garrett, W. E., Jr. (1996). Muscle strain injuries. *The American Journal of Sports Medicine*, *24*(6 Suppl), S2–S8.

Garrett, W. E., Jr, Califf, J. C., & Bassett, F. H., 3rd. (1984). Histochemical correlates of hamstring injuries. *The American Journal of Sports Medicine*, *12*(2), 98–103.

Giavarina, D. (2015). Understanding Bland Altman analysis. *Biochemia Medica: Casopis Hrvatskoga Drustva Medicinskih Biokemicara / HDMB*, *25*(2), 141–151.

Giraudo, C., Motyka, S., Weber, M., Karner, M., Resinger, C., Feiweier, T., Bogner, W. (2018). Normalized STEAM-based diffusion tensor imaging provides a robust assessment of muscle tears in football players: preliminary results of a new approach to evaluate muscle injuries. *European Radiology*.

Gonçalves, B., Hegyi, A., Avela, J., & Cronin, N. (2017). Regional differences in biceps femoris fascicle length and pennation angle after a simulated soccer mactch. *British Journal of Sports Medicine*, *51*(4), 322.1–322.

Heckmatt, J. Z., Dubowitz, V., & Leeman, S. (1981). Ultrasound Imaging in the Diagnosis of Muscle Disease. *Clinical Science*, *60*(3), 19P.1–19P.

Heemskerk, A. M., Drost, M. R., van Bochove, G. S., van Oosterhout, M. F. M., Nicolay, K., & Strijkers, G. J. (2006). DTI-based assessment of ischemia-reperfusion in mouse skeletal muscle. *Magnetic Resonance in Medicine: Official Journal of the Society of Magnetic Resonance in Medicine / Society of Magnetic Resonance in Medicine*, *56*(2), 272–281.

Henkelman, R. M., Mark Henkelman, R., Stanisz, G. J., Kim, J. K., & Bronskill, M. J. (1994). Anisotropy of NMR properties of tissues. *Magnetic Resonance in Medicine: Official Journal of the Society of Magnetic Resonance in Medicine / Society of Magnetic Resonance in Medicine*, *32*(5), 592–601.

Herbert, R. D., & Gandevia, S. C. (1995). Changes in pennation with joint angle and muscle torque: in vivo measurements in human brachialis muscle. *The Journal of Physiology*, *484*(2), 523–532.

Hides, J. A., Stokes, M. J., Saide, M., Jull, G. A., & Cooper, D. H. (1994). Evidence of Lumbar Multifidus Muscle Wasting Ipsilateral to Symptoms in Patients with Acute/Subacute Low Back Pain. *Spine*, *19*(Supplement), 165–172.

Hodges, P. W., Pengel, L. H. M., Herbert, R. D., & Gandevia, S. C. (2003). Measurement of muscle contraction with ultrasound imaging. *Muscle & Nerve*, *27*(6), 682–692.

Hoffer, J. A., Caputi, A. A., Pose, I. E., & Griffiths, R. I. (1989). Chapter 7 Roles of muscle activity and load on the relationship between muscle spindle length and whole muscle length in the freely walking cat. In *Progress in Brain Research* (pp. 75–85).

Hopkins, W. G. (2000). Measures of reliability in sports medicine and science. *Sports Medicine* , *30*(1), 1–15.

Hoskins, W. T., & Pollard, H. P. (2005). Successful management of hamstring injuries in Australian Rules footballers: two case reports. *Chiropractic & Osteopathy*, *13*(1), 4.

Huijing, P. A. (1985). Architecture of the Human Gastrocnemius Muscle and Some Functional Consequences. *Cells, Tissues, Organs*, *123*(2), 101–107.

Huijing PhD, P. A., Huijing, P. A., & Langevin, H. M. (2009). Communicating About Fascia: History, Pitfalls, and Recommendations. *International Journal of Therapeutic Massage & Bodywork: Research, Education, & Practice*, *2*(4).

Ikai, M., & Fukunaga, T. (1968). Calculation of muscle strength per unit cross-sectional area of human muscle by means of ultrasonic measurement. *Internationale Zeitschrift Fur Angewandte Physiologie, Einschliesslich Arbeitsphysiologie*, *26*(1), 26–32.

Jukka Jauhiainen (2009). *The Physical Principles of Medical Imaging.* http://www.oamk.fi/~jjauhiai/opetus/mittalaitteet/US.pdf

Kawakami, Y., Abe, T., & Fukunaga, T. (1993). Muscle-fiber pennation angles are greater in hypertrophied than in normal muscles. *Journal of Applied Physiology*, *74*(6), 2740–2744.

Kellis, E. (2016). Biceps femoris and semitendinosus tendon/aponeurosis strain during passive and active (isometric) conditions. *Journal of Electromyography and Kinesiology: Official Journal of the International Society of Electrophysiological Kinesiology*, *26*, 111–119.

Kellis, E. (2018). Biceps femoris fascicle length during passive stretching. *Journal of Electromyography and Kinesiology: Official Journal of the International Society of Electrophysiological Kinesiology*, *38*, 119–125.

Kellis, E., Galanis, N., Kapetanos, G., & Natsis, K. (2012). Architectural differences between the hamstring muscles. *Journal of Electromyography and Kinesiology: Official Journal of the International Society of Electrophysiological Kinesiology*, *22*(4), 520–526.

Kellis, E., Galanis, N., Natsis, K., & Kapetanos, G. (2009). Validity of architectural properties of the hamstring muscles: Correlation of ultrasound findings with cadaveric dissection. *Journal of Biomechanics*, *42*(15), 2549–2554.

Kellis, E., Galanis, N., Natsis, K., & Kapetanos, G. (2010). Muscle architecture variations along the human semitendinosus and biceps femoris (long head) length. *Journal of Electromyography and Kinesiology: Official Journal of the International Society of Electrophysiological Kinesiology*, *20*(6), 1237–1243.

Kuitunen, S., Komi, P. V., & Kyröläinen, H. (2002). Knee and ankle joint stiffness in sprint running. *Medicine and Science in Sports and Exercise*, *34*(1), 166–173.

Kwah, L. K., Pinto, R. Z., Diong, J., & Herbert, R. D. (2013). Reliability and validity of ultrasound measurements of muscle fascicle length and pennation in humans: a systematic review. *Journal of Applied Physiology*, *114*(6), 761–769.

Lansdown, D. A., Ding, Z., Wadington, M., Hornberger, J. L., & Damon, B. M. (2007). Quantitative diffusion tensor MRI-based fiber tracking of human skeletal muscle. *Journal of Applied Physiology*, *103*(2), 673–681.

Lieber, R. L., & Fridén, J. (2000). Functional and clinical significance of skeletal muscle architecture. *Muscle & Nerve*, *23*(11), 1647–1666.

Maganaris, C. N., & Baltzopoulos, V. (1999). Predictability of in vivo changes in pennation angle of human tibialis anterior muscle from rest to maximum isometric dorsiflexion. *European Journal of Applied Physiology*, *79*(3), 294–297.

Makihara, Y., Nishino, A., Fukubayashi, T., & Kanamori, A. (2005). Decrease of knee flexion torque in patients with ACL reconstruction: combined analysis of the architecture and function of the knee flexor muscles. *Knee Surgery, Sports Traumatology, Arthroscopy: Official Journal of the ESSKA*, *14*(4), 310–317.

Mann, R., & Sprague, P. (1980). A kinetic analysis of the ground leg during sprint running. *Research Quarterly for Exercise and Sport*, *51*(2), 334–348.

Maughan, R. J., Watson, J. S., & Weir, J. (1983). Strength and cross-sectional area of human skeletal muscle. *The Journal of Physiology*, *338*(1), 37–49.

McKenzie, D. K., Gandevia, S. C., Gorman, R. B., & Southon, F. C. (1994). Dynamic changes in the zone of apposition and diaphragm length during maximal respiratory efforts. *Thorax*, *49*(7), 634–638.

Mero, A., & Komi, P. V. (1987). Electromyographic activity in sprinting at speeds ranging from sub-maximal to supra-maximal. *Medicine and Science in Sports and Exercise*, *19*(3), 266–274.

Misuri, G., Colagrande, S., Gorini, M., Iandelli, I., Mancini, M., Duranti, R., & Scano, G. (1997). In vivo ultrasound assessment of respiratory function of abdominal muscles in normal subjects. *The European Respiratory Journal: Official Journal of the European Society for Clinical Respiratory Physiology*, *10*(12), 2861–2867.

Morgan, D. L., Proske, U., & Warren, D. (1978). Measurements of muscle stiffness and the mechanism of elastic storage of energy in hopping kangaroos. *The Journal of Physiology*, *282*(1), 253–261.

Muhl, Z. F. (1982). Active length-tension relation and the effect of muscle pinnation on fiber lengthening. *Journal of Morphology*, *173*(3), 285–292.

Nakamura, M., Ikezoe, T., Takeno, Y., & Ichihashi, N. (2013). Time course of changes in passive properties of the gastrocnemius muscle–tendon unit during 5 min of static stretching. *Manual Therapy*, *18*(3), 211–215.

Narici, M. (1999). Human skeletal muscle architecture studied in vivo by non-invasive imaging techniques: functional significance and applications. *Journal of Electromyography and Kinesiology: Official Journal of the International Society of Electrophysiological Kinesiology*, *9*(2), 97–103.

Narici, M. V., Binzoni, T., Hiltbrand, E., Fasel, J., Terrier, F., & Cerretelli, P. (1996). In vivo human gastrocnemius architecture with changing joint angle at rest and during graded isometric contraction. *The Journal of Physiology*, *496*(1), 287–297.

Noorkoiv, M., Stavnsbo, A., Aagaard, P., & Blazevich, A. J. (2010). In vivo assessment of muscle fascicle length by extended field-of-view ultrasonography. *Journal of Applied Physiology*, *109*(6), 1974–1979.

Oliveira, V. B. de, de Oliveira, V. B., de Janeiro, U. F. do R., Brazil, Carneiro, S. P., de Oliveira, L. F., Brazil. (2016). Reliability of biceps femoris and semitendinosus muscle architecture measurements obtained with ultrasonography. *Research on Biomedical Engineering*, *32*(4), 365–371.

Opar, D. A., Williams, M. D., & Shield, A. J. (2012). Hamstring strain injuries: factors that lead to injury and re-injury. *Sports Medicine* , *42*(3), 209–226.

Orchard, J. W., Seward, H., & Orchard, J. J. (2013). Results of 2 decades of injury surveillance and public release of data in the Australian Football League. *The American Journal of Sports Medicine*, *41*(4), 734–741.

Otten, E. (1988). Concepts and models of functional architecture in skeletal muscle. *Exercise and Sport Sciences Reviews*, *16*, 89–137.

Potier, T. G., Alexander, C. M., & Seynnes, O. R. (2009). Effects of eccentric strength training on biceps femoris muscle architecture and knee joint range of movement. *European Journal of Applied Physiology*, *105*(6), 939–944.

Proske, U., Morgan, D. L., Brockett, C. L., & Percival, P. (2004). IDENTIFYING ATHLETES AT RISK OF HAMSTRING STRAINS AND HOW TO PROTECT THEM. *Clinical and Experimental Pharmacology and Physiology*, *31*(8), 546–550.

Reeves, N. D., Maganaris, C. N., & Narici, M. V. (2004). Ultrasonographic assessment of human skeletal muscle size. *European Journal of Applied Physiology*, *91*(1), 116–118.

Ribeiro-Alvares, J. B., Marques, V. B., Vaz, M. A., & Baroni, B. M. (2018). Four Weeks of Nordic Hamstring Exercise Reduce Muscle Injury Risk Factors in Young Adults. *Journal of Strength and Conditioning Research / National Strength & Conditioning Association*, *32*(5), 1254–1262.

Rutherford, O. M., & Jones, D. A. (1992). Measurement of fibre pennation using ultrasound in the human quadriceps in vivo. *European Journal of Applied Physiology and Occupational Physiology*, *65*(5), 433–437.

Sacks, R. D., & Roy, R. R. (1982). Architecture of the hind limb muscles of cats: functional significance. *Journal of Morphology*, *173*(2), 185–195.

Sá, M. A., Matta, T. T., Carneiro, S. P., Araujo, C. O., Novaes, J. S., & Oliveira, L. F. (2016). Acute Effects of Different Methods of Stretching and Specific Warm-ups on Muscle Architecture and Strength Performance. *Journal of Strength and Conditioning Research / National Strength & Conditioning Association*, *30*(8), 2324–2329.

Saotome, T., Sekino, M., Eto, F., & Ueno, S. (2006). Evaluation of diffusional anisotropy and microscopic structure in skeletal muscles using magnetic resonance. *Magnetic Resonance Imaging*, *24*(1), 19–25.

Seidel, P. M., Seidel, G. K., Gans, B. M., & Dijkers, M. (1996). Precise localization of the motor nerve branches to the hamstring muscles: an aid to the conduct of neurolytic procedures. *Archives of Physical Medicine and Rehabilitation*, *77*(11), 1157–1160.

Seymore, K. D., Domire, Z. J., DeVita, P., Rider, P. M., & Kulas, A. S. (2017). The effect of Nordic hamstring strength training on muscle architecture, stiffness, and strength. *European Journal of Applied Physiology*, *117*(5), 943–953.

Sheskin, D. J. (2000). *Handbook of Parametric and Nonparametric Statistical Procedures: Second Edition*. Chapman and Hall/CRC.

Silder, A., Heiderscheit, B. C., Thelen, D. G., Enright, T., & Tuite, M. J. (2008). MR observations of long-term musculotendon remodeling following a hamstring strain injury. *Skeletal Radiology*, *37*(12), 1101–1109.

Silder, A., Reeder, S. B., & Thelen, D. G. (2010). The influence of prior hamstring injury on lengthening muscle tissue mechanics. *Journal of Biomechanics*, *43*(12), 2254–2260.

Sinha, S., Sinha, U., & Edgerton, V. R. (2006). In vivo diffusion tensor imaging of the human calf muscle. *Journal of Magnetic Resonance Imaging: JMRI*, *24*(1), 182–190.

Stanton, P., & Purdam, C. (1989). Hamstring Injuries in Sprinting—The Role of Eccentric Exercise. *The Journal of Orthopaedic and Sports Physical Therapy*, *10*(9), 343–349.

Thelen, D. G., Chumanov, E. S., Hoerth, D. M., Best, T. M., Swanson, S. C., Li, L., … Heiderscheit, B. C. (2005). Hamstring muscle kinematics during treadmill sprinting. *Medicine and Science in Sports and Exercise*, *37*(1), 108–114.

Timmins, R. G., Bourne, M. N., Shield, A. J., Williams, M. D., Lorenzen, C., & Opar, D. A. (2016). Biceps Femoris Architecture and Strength in Athletes with a Previous Anterior Cruciate Ligament Reconstruction. *Medicine and Science in Sports and Exercise*, *48*(3), 337–345.

Timmins, R. G., Bourne, M. N., Shield, A. J., Williams, M. D., Lorenzen, C., & Opar, D. A. (2016). Short biceps femoris fascicles and eccentric knee flexor weakness increase the risk of hamstring injury in elite football (soccer): a prospective cohort study. *British Journal of Sports Medicine*, *50*(24), 1524–1535.

Timmins, R. G., Ruddy, J. D., Presland, J., Maniar, N., Shield, A. J., Williams, M. D., & Opar, D. A. (2016). Architectural Changes of the Biceps Femoris Long Head after Concentric or Eccentric Training. *Medicine & Science in Sports & Exercise*, *48*(3), 499–508.

Timmins, R. G., Shield, A. J., Williams, M. D., Lorenzen, C., & Opar, D. A. (2015). Biceps femoris long head architecture: a reliability and retrospective injury study. *Medicine and Science in Sports and Exercise*, *47*(5), 905–913.

Tosovic, D., Muirhead, J. C., Brown, J. M. M., & Woodley, S. J. (2016). Anatomy of the long head of biceps femoris: An ultrasound study. *Clinical Anatomy* , *29*(6), 738–745.

Turner, A. N., Cree, J., Comfort, P., Jones, L., Chavda, S., Bishop, C., & Reynolds, A. (2014). Hamstring Strain Prevention in Elite Soccer Players. *Strength and Conditioning Journal*, *36*(5), 10–20.

van der Made, A. D., Wieldraaijer, T., Kerkhoffs, G. M., Kleipool, R. P., Engebretsen, L., van Dijk, C. N., & Golanó, P. (2015). The hamstring muscle complex. *Knee Surgery, Sports Traumatology, Arthroscopy: Official Journal of the ESSKA*, *23*(7), 2115–2122.

Verrall, G. M., Slavotinek, J. P., Barnes, P. G., Fon, G. T., & Esterman, A. (2006). Assessment of physical examination and magnetic resonance imaging findings of hamstring injury as predictors for recurrent injury. *The Journal of Orthopaedic and Sports Physical Therapy*, *36*(4), 215–224.

Wickiewicz, T. L., Roy, R. R., Powell, P. L., & Edgerton, V. R. (1983). Muscle architecture of the human lower limb. *Clinical Orthopaedics and Related Research*, (179), 275–283.

Wickiewicz, T. L., Roy, R. R., Powell, P. L., Perrine, J. J., & Edgerton, V. R. (1984). Muscle architecture and force-velocity relationships in humans. *Journal of Applied Physiology: Respiratory, Environmental and Exercise Physiology*, *57*(2), 435–443.

Wood, G. (1987). Biomechanical Limitations to Sprint Running. *Med. Sci. Sports Exerc.*, *25*, 58–71.

Woodley, S. J., & Mercer, S. R. (2005). Hamstring Muscles: Architecture and Innervation. *Cells, Tissues, Organs*, *179*(3), 125–141.

Woods, C., Hawkins, R. D., Maltby, S., Hulse, M., Thomas, A., Hodson, A., & Football Association Medical Research Programme. (2004). The Football Association Medical Research Programme: an audit of injuries in professional football--analysis of hamstring injuries. *British Journal of Sports Medicine*, *38*(1), 36–41.

Wu, M.-T., Tseng, W.-Y. I., Su, M.-Y. M., Liu, C.-P., Chiou, K.-R., Wedeen, V. J., Yang, C.-F. (2006). Diffusion tensor magnetic resonance imaging mapping the fiber architecture remodeling in human myocardium after infarction: correlation with viability and wall motion. *Circulation*, *114*(10), 1036–1045.

Yang L., Zhang M.-Z., Zhang W., Zhao Y.-L., & Zhao J.-Z. (2006). [Application of diffusion tensor imaging fractography in minimally invasive surgery of brain tumors]. *Zhonghua yi xue za zhi*, *86*(19), 1301–1304.

Zaraiskaya, T., Kumbhare, D., & Noseworthy, M. D. (2006). Diffusion tensor imaging in evaluation of human skeletal muscle injury. *Journal of Magnetic Resonance Imaging: JMRI*, *24*(2), 402–408.

**APPENDIX**

Suplemental Data

| | Fascicle Length (mm) | | | | Fascicle Length (mm) | | | Absolute ranking diference | |
|---|---|---|---|---|---|---|---|---|---|
| Individuals | Static | Linear-EFOV | Nonlinear-EFOV | Ranking-Static | Static | Linear-EFOV | Nonlinear-EFOV | DIF S-L | DIF S-NL |
| 1 | 70,10 | 70,60 | 57,90 | 1 | 66,12 | 63,70 | 57,90 | 0 | 1 |
| 2 | 88,70 | 73,90 | 77,55 | 2 | 70,10 | 66,77 | 64,70 | 5 | 1 |
| 3 | 95,70 | 92,70 | 90,90 | 3 | 73,05 | 67,40 | 67,25 | 0 | 2 |
| 4 | 75,20 | 68,20 | 71,95 | 4 | 75,20 | 68,20 | 70,35 | 0 | 2 |
| 5 | 79,95 | 76,70 | 82,95 | 5 | 75,50 | 68,95 | 71,82 | 1 | 5 |
| 6 | 73,05 | 67,40 | 71,82 | 6 | 76,50 | 70,05 | 71,95 | 4 | 3 |
| 7 | 84,25 | 73,55 | 76,18 | 7 | 79,75 | 70,60 | 73,63 | 2 | 3 |
| 8 | 83,55 | 81,25 | 81,55 | 8 | 79,95 | 73,15 | 76,18 | 5 | 8 |
| 9 | 75,50 | 70,05 | 77,23 | 9 | 82,05 | 73,55 | 77,20 | 3 | 6 |
| 10 | 106,65 | 89,15 | 91,45 | 10 | 83,00 | 73,62 | 77,23 | 0 | 1 |
| 11 | 87,73 | 77,25 | 73,63 | 11 | 83,55 | 73,90 | 77,55 | 6 | 2 |
| 12 | 82,05 | 75,20 | 82,70 | 12 | 83,73 | 75,20 | 78,37 | 4 | 0 |
| 13 | 108,30 | 81,00 | 84,40 | 13 | 84,25 | 76,70 | 81,55 | 4 | 5 |
| 14 | 79,75 | 68,95 | 70,35 | 14 | 87,73 | 77,25 | 81,80 | 0 | 7 |
| 15 | 76,50 | 66,77 | 67,25 | 15 | 88,70 | 79,85 | 82,70 | 4 | 4 |
| 16 | 103,65 | 89,65 | 90,60 | 16 | 95,00 | 81,00 | 82,95 | 1 | 2 |
| 17 | 83,00 | 73,62 | 77,20 | 17 | 95,70 | 81,25 | 84,40 | 3 | 2 |
| 18 | 83,73 | 73,15 | 78,37 | 18 | 103,65 | 89,15 | 90,60 | 1 | 0 |
| 19 | 95,00 | 79,85 | 81,80 | 19 | 106,65 | 89,65 | 90,90 | 1 | 1 |
| 20 | 66,12 | 63,70 | 64,70 | 20 | 108,30 | 92,70 | 91,45 | 4 | 3 |
| | | | | | | | **Mean** | **2,4** | **2,9** |
| | | | | | | | **SD** | 2,0 | 2,3 |